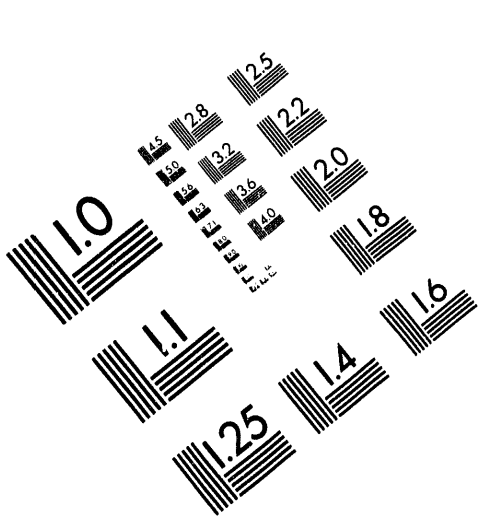

**Association for Information and Image Management**

1100 Wayne Avenue, Suite 1100
Silver Spring, Maryland 20910

301/587-8202

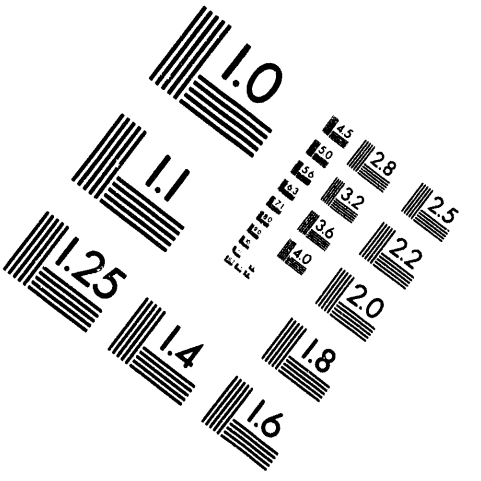

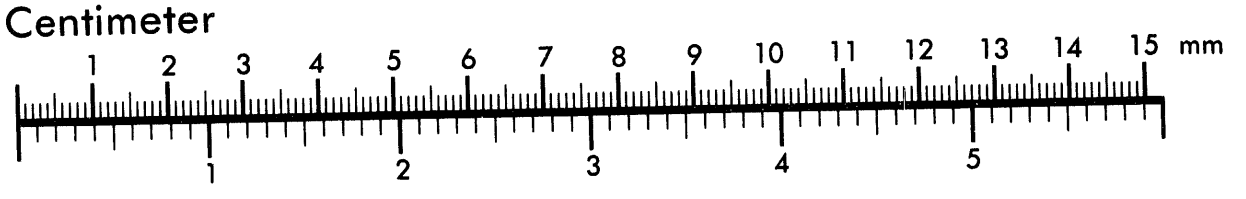


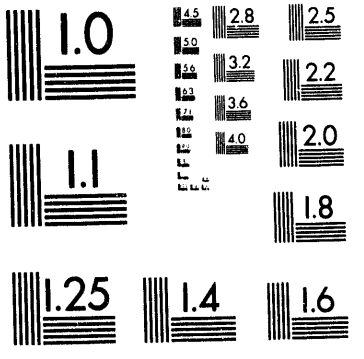

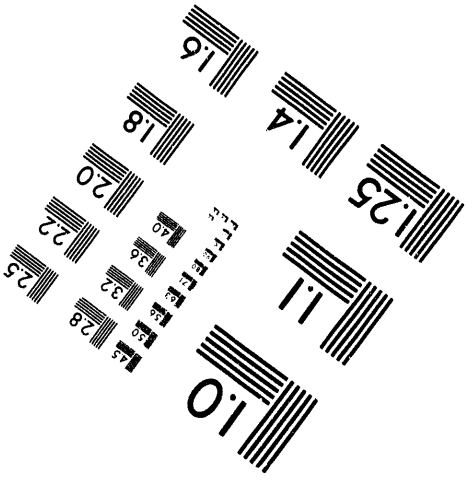

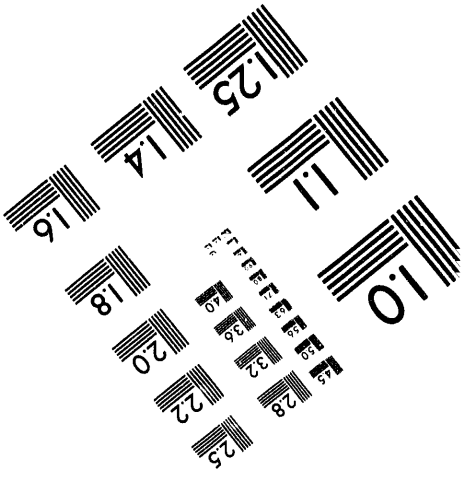

1 of 1

**BIRL**

Industrial Research Laboratory
1801 Maple Avenue
Evanston, Illinois 60201-3135

Argonne National Laboratory
Contract No. 00732401

**FINAL REPORT**

# TRIBOLOGICAL PROPERTIES OF REACTIVELY SPUTTERED NITRIDES AND CARBIDES OF TITANIUM, ZIRCONIUM AND HAFNIUM

**FOR**

by

Michael E. Graham
Research Scientist

Peter Chang
Research Scientist

W. D. Sproul
Group Leader

May 10, 1994

## TABLE OF CONTENTS



## LIST OF TABLES



## LIST OF FIGURES

## INTRODUCTION AND SUMMARY

The purpose of this study was to determine the tribological properties of hard, wear-resistant coatings on steel substrates in order to expedite the use of these materials on engineered surfaces such as coated roller bearings, transmission gears, and cams. The specific coatings to be investigated for the Department of Energy (DOE) project were the carbides and nitrides of titanium, zirconium, and hafnium (TiN, TiC, ZrN, ZrC, HfN, and HfC). All the coatings were deposited by high-rate-reactive magnetron sputtering (HRRS), which was developed by Dr. Wiliiam D. Sproul.

The original goals of the project included increasing the knowledge base regarding the friction and wear behavior of these coatings so that engineers would have enough information to anticipate the potential benefits of coating engineering surfaces for various wear applications. The first task area involved development of the coating process for the six coatings on the selected substrates (typically 52100 steel, hardened to Rc 62) and characterization of the coated samples. This effort required determination of the operating conditions needed to obtain the best adhesion and the best hardness for each coating. Hardness and adhesion were critical properties for selecting the conditions to be used for coating wear test samples.

Where possible, the coatings were deposited at the highest rate possible (consistent with good adhesion and hardness). The use of statistically designed experiments (SDE's) was an important factor in obtaining the best information with the fewest number of coating experiments. The results were used in response surface plots to display the parametric effects. X-ray diffraction was used to determine the crystallographic phases present and the growth texture. Some idea of the elastic strain induced by the process could also be deduced from the deviation in the measured lattice parameters from the published equilibrium values.

Task 2 involved tribological testing of the coated samples (TiN, TiC, ZrN, ZrC, HfN, and HfC). Northwestern University's two-disc wear tester was used to determine the rolling contact fatigue behavior of TiN coated samples.

Optical microscopy and SEM analysis were used to investigate the nature of surface and subsurface crack development during the test. Although it was not possible to perform the fatigue type tests on the other coatings, they were subjected to scuffing failure tests using the variable roll-slide equipment and to pin-on-disc tests. These other tests broadened the scope of testing that was done but lead to a better understanding of the effects of the deposition parameters and substrate properties on the overall performance of coated steel.

The tribology group at Argonne National Laboratory, tested some of the coatings made at BIRL as a part of the program. The tests run at ANL were pin-on-disc (room temperature to 400°C) and oscillating slider tests which simulate different wear modes. Some of this work was reported in a paper for the ICMC in 1991.[1] ANL was not able to conduct all of the tests originally planned due to a lack of manpower and funding.

The third task was originally designed to investigate the effects of doping on the wear resistance of the nitrides studied here. The use of dopants such as As, Sb, and Bi had previously been shown to increase the hardness of the nitrides significantly, and the effect of this increased hardness on wear resistance was to be measured. However, as DOE funding priorities changed, the third task area had to be abandoned.

The work reviewed in this document was all presented in quarterly reports issued over the period 1990 to 1993 by DOE. This report will not cover the tribological details as thoroughly as the previous reports but will collect and review the main results and the relevant discussions. The deposition work will be covered since it was not as fully reported as the wear testing.

## RESULTS AND DISCUSSION

### Coating Deposition

#### TiN

We were familiar with the deposition conditions for TiN from our past experience, and we were able to minimize the time needed to develop the operating parameters. The characterization of TiN was also more complete in

previous work than for the other materials. It was therefore possible to devote more time to exploring the performance of the TiN coatings and the dependence of that performance on the deposition parameters. Due to these investigations with TiN, we became aware of the strong dependence of wear behavior on coating thickness, hardness, and adhesion, which are controlled by the process parameters, and on the nature of the substrate itself. We realized the importance of looking at the other coating materials in terms of their deposition parameters as well. Thus, much of the wear testing was designed specifically to differentiate the performance of coatings made under different values of operating parameters such as partial pressure of the reactive gas or substrate bias voltage.

Typical deposition parameters for TiN, along with the associated properties, are as follows:

**Deposition Parameters**

Partial Pressure = $1.6 \times 10^{-4}$ Torr (0.16 mTorr)
Total Pressure = 8.0 mTorr
Substrate Bias = (-) 100 - 150 V
Target Power = 10 kW (dc)
Deposition Rate = 0.48-0.5 $\mu$m/min

**Coating Properties**

Hardness = 2000-2400 kgf/mm$^2$ (Vickers, 25gm load)
Adhesion = 5.0-6.0 kgf (critical load, 5-$\mu$m thick)
Lattice Parameter = 4.26-4.28 Å

As with all the reactively sputtered compounds we tested, the work began by defining the hysteresis curve (under partial pressure control), which relates the partial pressure of nitrogen to the flow rate of nitrogen. This curve shows where there is a significant formation of nitride on the target as well as on the substrate, and consequently, a reduced deposition rate. It is evident from the curve in Figure 1 that certain regimes of partial pressure are only accessible if one is operating in the partial-pressure-control mode. Figure 1 is a typical hysteresis curve for TiN made under partial-pressure control. The use of flow control is inadequate since a flow set-point in the

region around the knee of the curve can actually correspond to any of two or three nitrogen partial pressures.

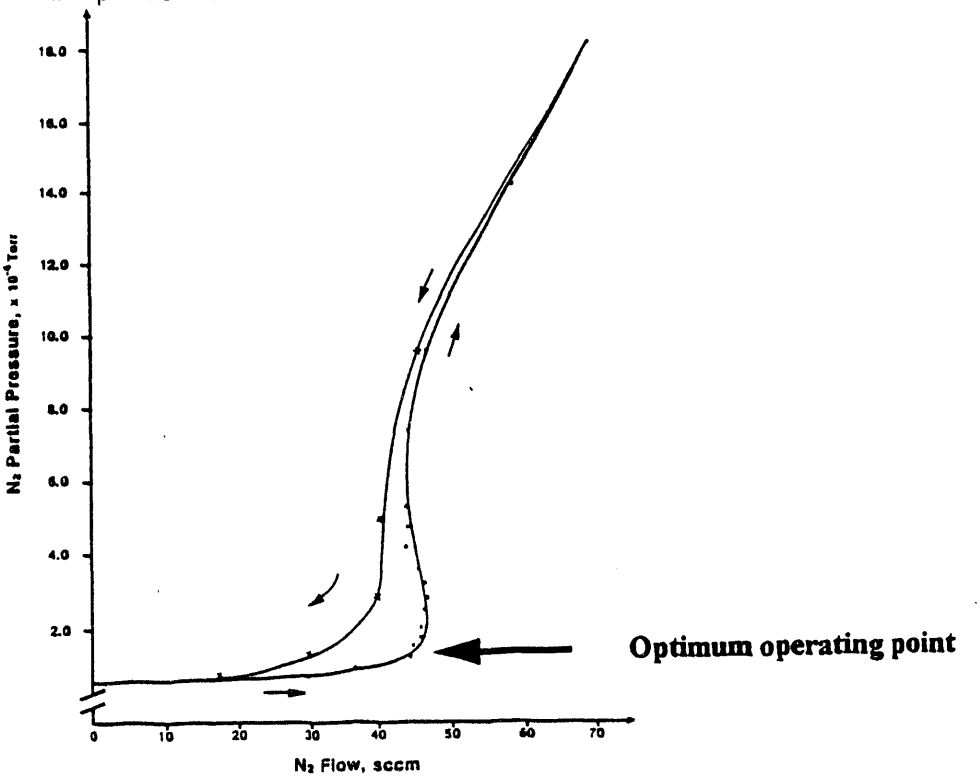


**Figure 1. TiN Hysteresis Curve - Partial Pressure Control**

Process fluctuations generally cause the system to shift to the higher partial pressures and the deposition rate to drop accordingly. We can determine the best operating parameters by exploring the region above and below the knee of the curve at any given power. This region of the curve corresponds to the highest consumption of nitrogen and also to the highest deposition rate.

In general, the best operating point has been found near the "knee" of the curve. However, the exact relative position on the curve varies from one compound to another. TiN has a "best" operating point just slightly below the knee of the curve.

## TiC

The deposition of TiC has also been characterized in the past, and it was known that partial pressure control was not necessary, since the curve relating partial pressure to the flow rate of methane ($CH_4$) did not exhibit

any region of negative slope. This monotonic dependency of flow on partial pressure is typical of carbide deposition for Ti, Zr, and Hf, whereas, the deposition of the respective nitrides always required partial pressure control. The flow rate of methane used in past work was about 40 sccm with 10 kW of power, at a total pressure of 8 mTorr.

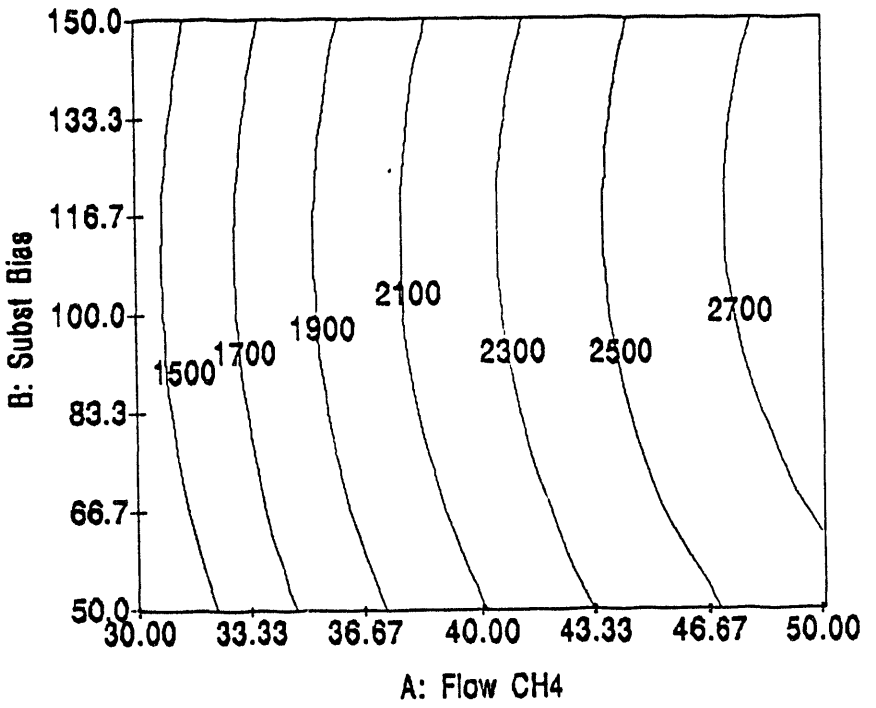


**Figure 2. Response Surface Plot - Hardness of TiC (VHN) vs. Flow Rate of $N_2$ (SCCM) and Substrate Bias (-V)**

A statistical-design study was run to confirm the best operating conditions in terms of optimum hardness and adhesion. While the adhesion was not very responsive to changes in parameters for the range of data taken, the hardness was very much dependent, in a regular and predictable way. The response surface plot in Figure 2 shows that the hardness changes from about 1500 VHN to 2800 VHN over the ranges of parameters investigated. (Only the flow rate and the substrate bias were varied in this set of experiments). The bias has only a minor effect, while the flow rate (amount of nitrogen available) has the major impact on hardness. This is consistent with the fact that TiC

exists over quite a wide range of composition (32-48 at.% @ 2000°C). Thus, as the lattice accommodates more and more carbon (up to 48%), it becomes harder and harder.

Similarly, the rate of deposition depends in an inverse way on the flow rate of methane. Figure 3 shows how the deposition rate decreases with increasing flow of $CH_4$. Interestingly, there seems to be a significant correlation of bias with deposition rate. While the statistical correlation of the data was good, it is not clearly understood why the highest rates should occur at the highest bias, and it is still possible that the few data points used to generate the response surface model could produce a false impression. This observation may warrant further investigation at another time.

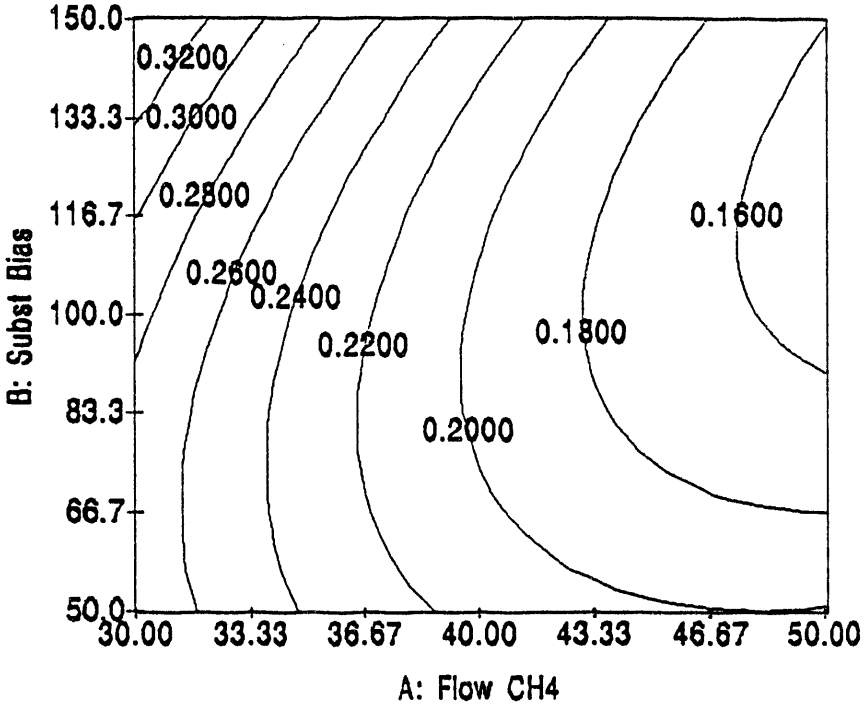


**Figure 3. Response Surface Plot - Deposition Rate of TiC ($\mu$m/min) vs. Flow Rate of $CH_4$ (SCCM)**

X-ray diffraction was also used to confirm the structure of the TiC and its lattice parameter. Figure 4 shows that the lattice parameter (measured value

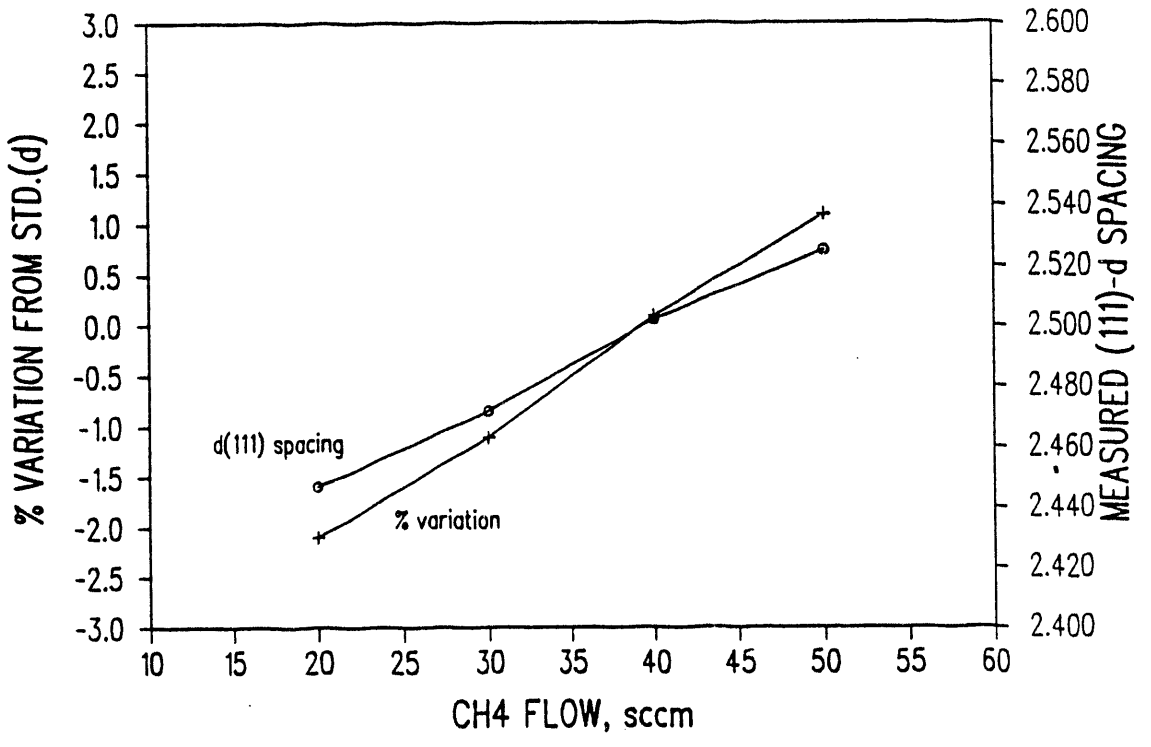


**Figure 4. TiC d(111) Spacing vs. Flow Rate of $CH_4$ (SCCM)**

of d(111) increases with increasing methane flow. We have plotted both the measured d-spacing and the difference between the measured value and the JCPDS value. The measured value is nearly equal to the accepted value at about 40 sccm but this does not imply stoichiometry at this flow rate. At this point the film is probably sub-stoichiometric, and the measured d-spacing is affected by strain in the film. The coatings used for these X-ray measurements were 2.5-5.0 $\mu$m thick, and exhibited adhesion values as shown in Figure 5, normalized by thickness. The adhesion was a maximum at 40 sccm, with a critical load of 7.5 kgf for a 3.7-$\mu$m thickness. In light of other measurements we have made, this value seems a bit too high and may be due to the condition of the diamond indenter. Other measured values indicate that the scratch adhesion Lc would be 1 or 2 kgf lower, but the relative behavior is correct.

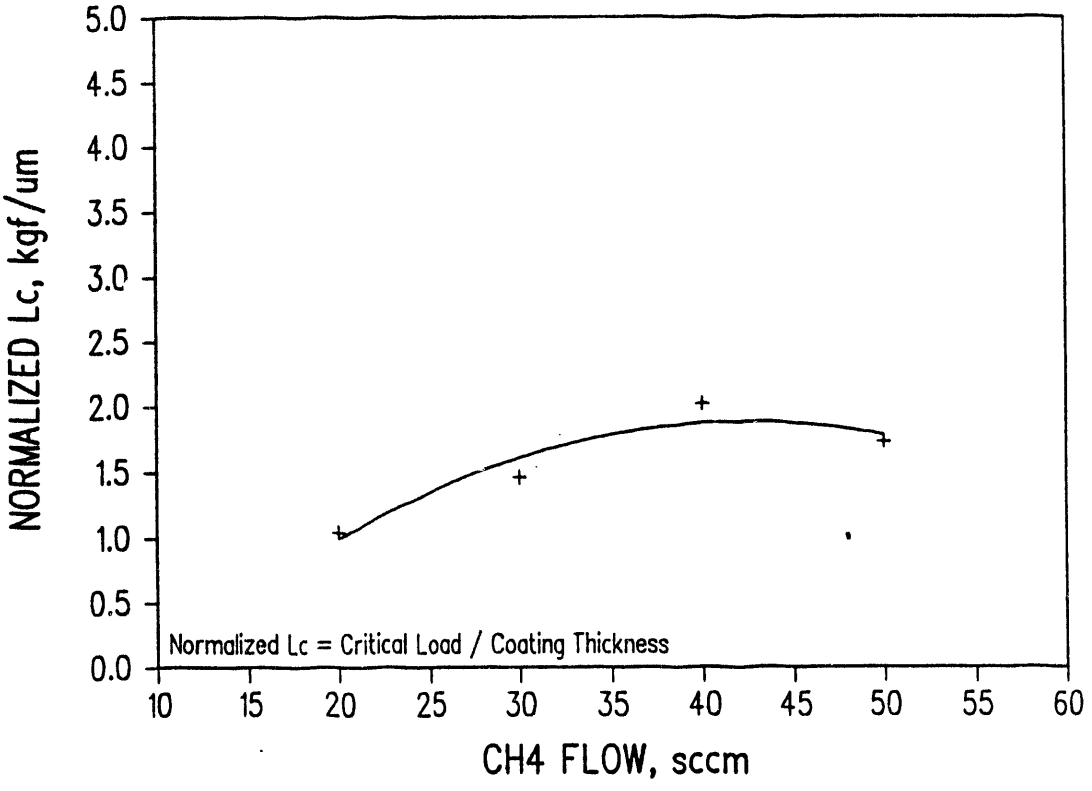


**Figure 5. Adhesion Critical Load for TiC on Steel vs. Flow Rate of $CH_4$**

ZrN

The approach for ZrN was very similar. In this investigation we also made use of the statistically designed experiments so that we could vary several parameters at one time and analyze the response functions to obtain optimum values of hardness and adhesion. We measured hardness and adhesion (as well as rate), and the correlation of the response data with the parameter settings was good. The control parameters were target power, substrate bias voltage, and nitrogen partial pressure. The total pressure was held constant at 8 mTorr for most of the work since this was known to be a good operating level and one that allowed wide variation in the other operating parameters.

Figure 6 shows the partial pressure-flow rate behavior for ZrN, sputtered at three different target powers (5, 8, and 10 kW). These curves were obtained

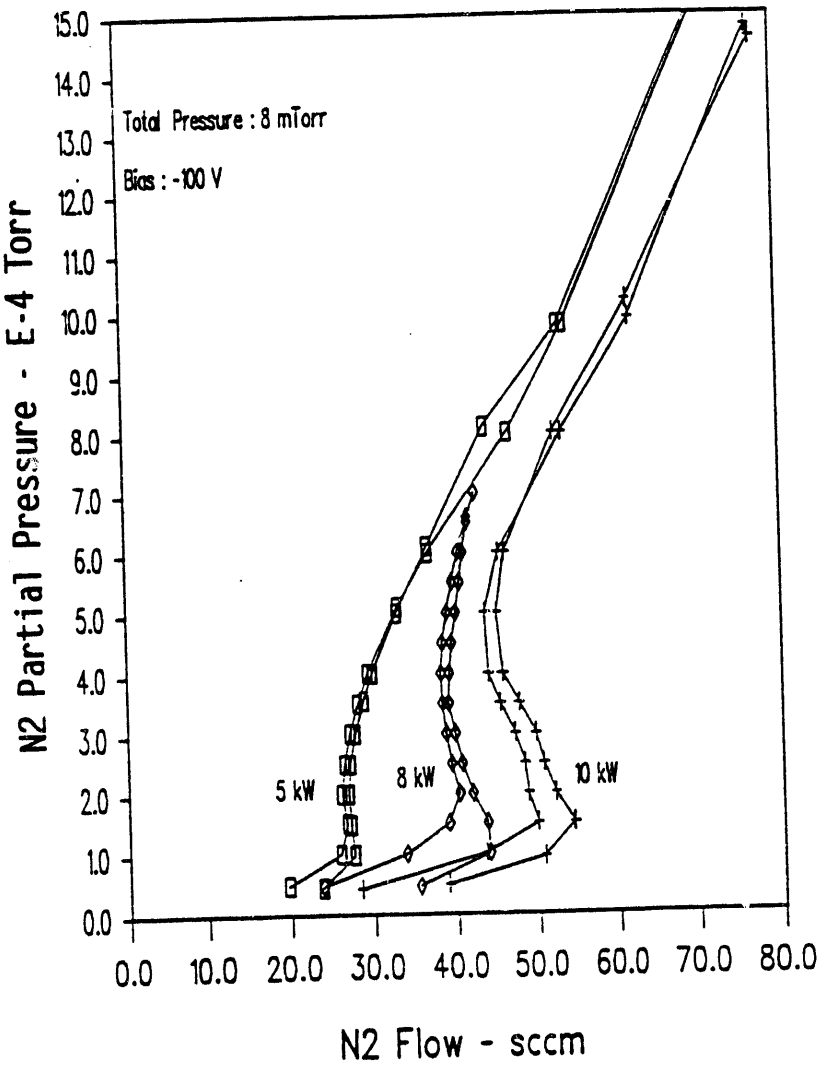


**Figure 6. ZrN Hysteresis Curves - Partial Pressure Control**

using partial pressure control so that the flow is actually the dependent variable. Of course, the flow rates increase in proportion to the increase in target power. The partial pressure of nitrogen at comparable points on the curves increases with power also, but less than proportionately.

As noted in the discussion of TiN, it is evident from the curves that certain regimes of partial pressure are only accessible if one is operating in the partial-pressure-control mode. We used the response surface technique to investigate the best operating conditions, using the ranges for the control parameters given below.

The power and the total pressure were held constant at values of 8 kW and 8 mTorr, respectively. The partial pressure and the substrate bias were varied to attain the best combination of hardness and adhesion in the range selected. The rate of deposition varies strongly with the partial pressure of nitrogen as seen in Figure 7. It would also be a strong function of power, but this dependency was not investigated since it should scale approximately linearly with the power. The rate contours show that the maximum rate (0.5 $\mu$m/min) is at low partial pressure, and decreases to about 0.35 $\mu$m/min at the highest partial pressure investigated.

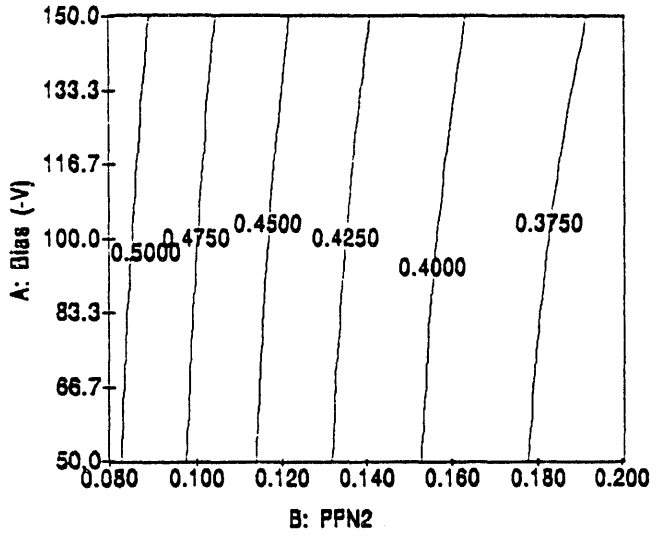


**Figure 7. Deposition Rate of ZrN vs. Partial Pressure of Nitrogen (m Torr) and Substrate Bias (-V)**

As seen in the following figures, the hardness and adhesion (on polished M2 steel) are more complicated functions of the partial pressure and bias. Figures 8a and 8b show the response contour plot for adhesion and hardness as functions of the variables. It is evident that there is a relative maximum for each variable in the regime investigated. The scratch-test critical load for adhesion yielded a maximum of 6.5 kgf in the ranges: $ppN_2$ = 1.5-1.9 x $10^{-4}$ Torr and bias = (-) 65-115 V. The bulls-eye for hardness was seen in Figure 8b to give a maximum of 2250 VHN in the ranges: $ppN_2$ = 1.3-1.75 x $10^{-4}$ Torr and a bias of (-) 80-140 V. Thus, it is possible to find considerable overlapping in the areas where both hardness and adhesion are high. This should provide coatings that give good abrasive and adhesive wear resistance.

While the plots in Figures 8a and 8b are modeled from the results of the statistically designed experiment, other data that was taken at constant

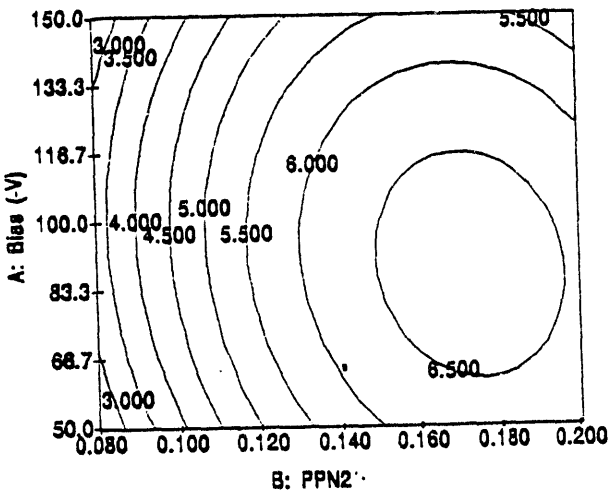


Figure 8a. Response Surface Plot - Adhesion (kgf) vs. Partial Pressure (x $10^{-4}$Torr) of $N_2$ and Bias (-V)

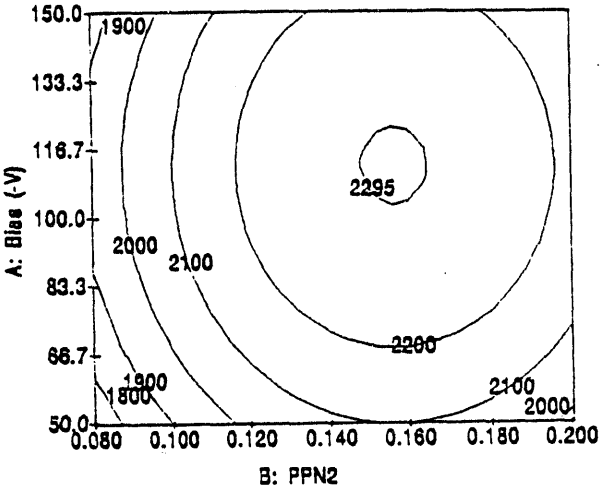


Figure 8b. Response Surface Plot - Hardness (VHN) vs. Partial Pressure (x$10^{-4}$Torr) of $N_2$ and Bias (-V)

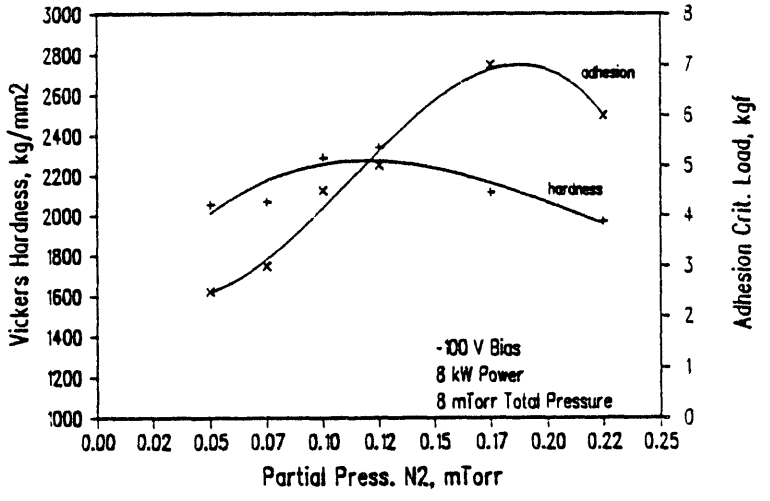


Figure 9. Hardness and Adhesion of ZrN vs. Partial Pressure of $N_2$

power, pressure and substrate bias are shown in Figure 9. This is equivalent to sectioning through the response surfaces at the -100 V-bias level, (keeping in mind that the correlation is not exact between the modeled response surface

and the line plot). This data also shows the broad maximum in hardness as a function of partial pressure ($N_2$), and it shows a shift to higher partial pressures for the adhesion maximum.

X-ray results indicate that the coatings are all the fcc phase with strong (111) and (200) reflections. The (111) and (200) diffraction peaks are very dominant for 5-$\mu$m thick films and have comparable magnitudes. For coatings that are less than 1 $\mu$m thick, the (111) and (200) peaks reduce in size by nearly an order of magnitude and are comparable with the (220) peak. The value of the ZrN lattice parameter was measured as a function of partial pressure and found to be quite insensitive to the partial pressure in the range used. This is in contrast to the behavior of TiN, where the lattice parameter increases with nitrogen content. The strain in the lattice of the deposited films is about 1.0%, based on the difference in lattice parameter measured and that given in the JCPDS cards (4.62 Å and 4.574 Å, respectively). Figure 10 shows a typical diffraction plot for a 5-$\mu$m

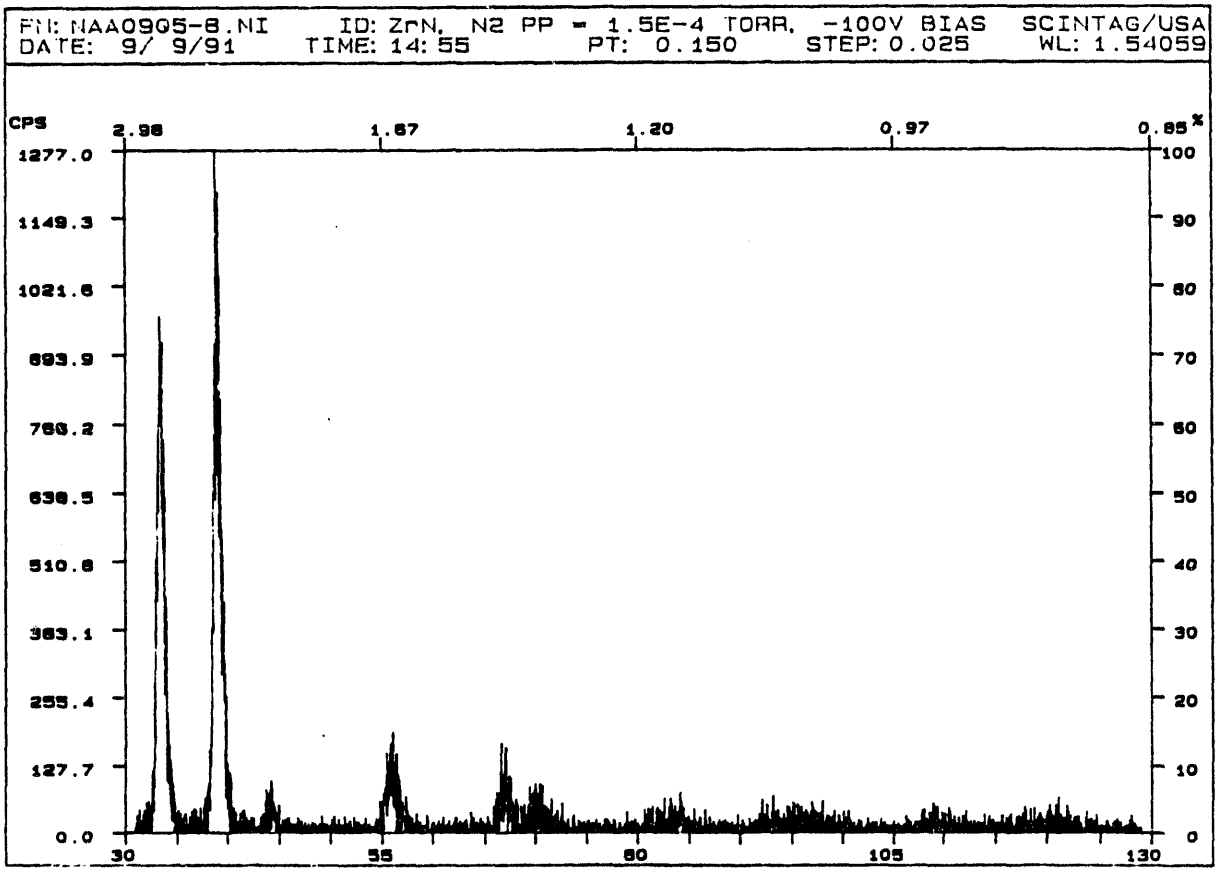


Figure 10. X-ray Diffraction Pattern for ZrN (typical)

thick film made using 8 kW of power at a total pressure of 8 mTor. The diffraction pattern shows typical preferred orientation with strong peaks for the (111) and (200) reflections.

## ZrC

The deposition of zirconium carbide was carried out in the dual-opposed-cathode system, using flow control instead of partial pressure control for the carbon bearing gas (similar to the case of TiC). Good quality films were difficult to make (in terms of adhesion) with methane. The hydrogen production from the methane made it difficult to maintain adequate control of gas flows and pressures. A change to acetylene was made in order to reduce the hydrogen production. The process was also sensitive to the amount of water vapor in the system, and steps were taken to minimize this contaminant. The carbide deposition appears to be much more sensitive than the nitride deposition to these factors. Deposition quality also deteriorated rapidly as the chamber and fixtures were coated. Maintaining good deposition conditions for the carbide was more difficult in general than it was for the nitride.

Successful ZrC was deposited using an interlayer of ZrN for adhesion. This technique was learned from previous experience (Sproul)[2]. The hardness ranged from about 1700 to 3000 Vickers, depending on the flow rate of $C_2H_2$, with a maximum in hardness occurring at a flow rate of 45 sccm. Figure 11

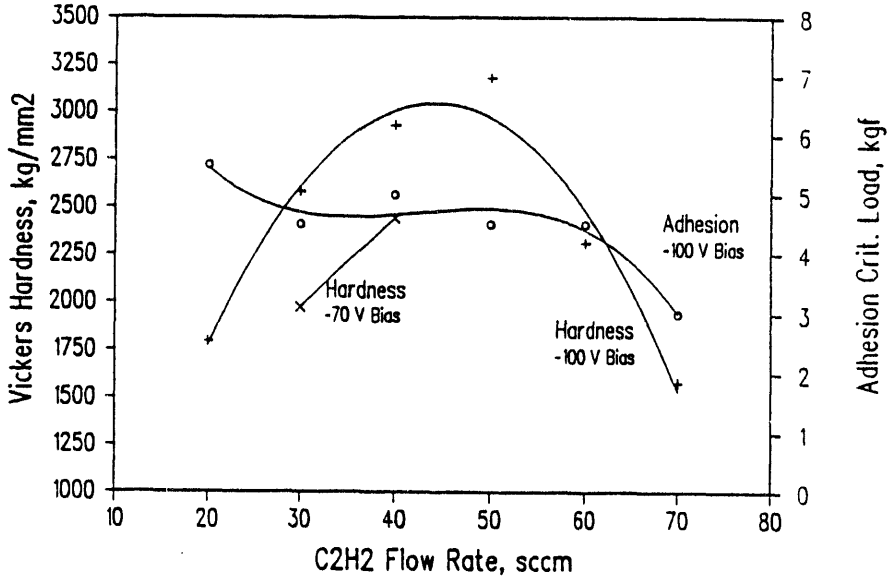


**Figure 11. Hardness and Adhesion of ZrC vs. Flow Rate of $C_2H_2$**

shows the responses of hardness and adhesion as a function of the flow rate of acetylene. While the hardness shows a clear maximum in the range of 40-50 sccm, the adhesion is not very sensitive to flow in this range. Only the low-flow condition produced better adhesion, but the 4.5 - 5.0 kgf critical load is good for films that are about 5 $\mu$m thick. It may be the effect of the ZrN interlayer that makes the adhesion relatively independent of the flow conditions.

A couple of runs were made using a lower bias (-70 V), and these values are plotted in the figure as well. The hardness is significantly reduced from the corresponding values at -100 V bias. The adhesion for these two coatings was measured at 3.5 and 6.0 kgf for the 30 and 40 sccm cases, respectively.

We have also characterized the coatings using X-ray diffraction. Within the range of acetylene flow explored, the cubic phase of ZrC was formed. The lattice parameter, plotted in Figure 12 as the $d_{(111)}$ spacing, did not change

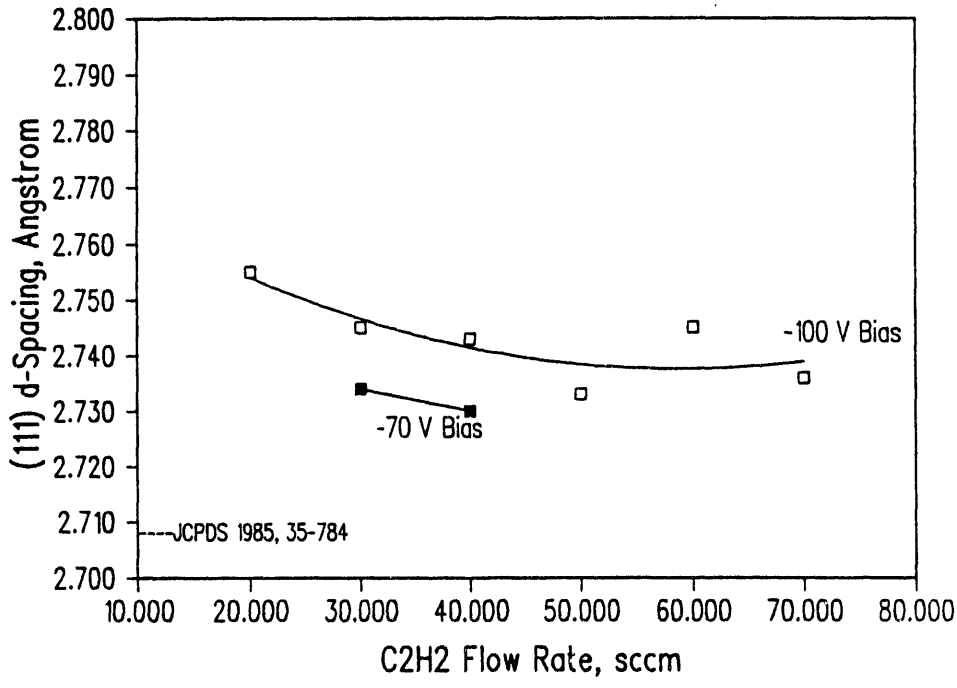


**Figure 12. ZrC d(111) Spacing vs. Flow Rate of $C_2H_2$**

much with acetylene flow but showed only a slight decline with increasing flow. The JCPDS value is given on the plot as well. As is usually observed with these coatings, the sputtered film has a larger d-spacing (by 1.3 - 1.5%), indicating a compressive stress. The higher-bias films also have higher stresses than the lower-bias films, as expected. Figure 13 shows a typical X-ray diffraction plot for the ZrC films. Again, there is a strong texture effect, with only a couple of dominant peaks.

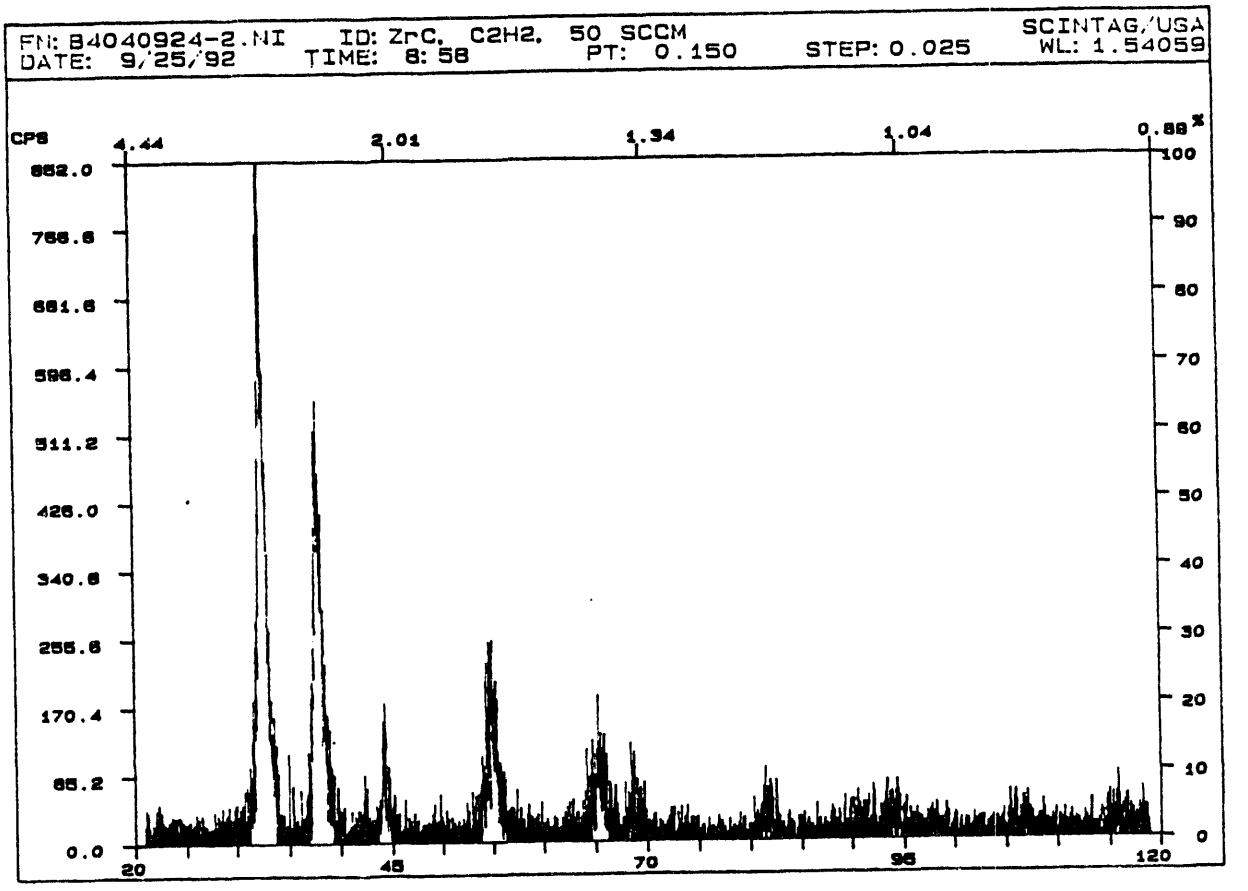


Figure 13. X-ray Diffraction Pattern for ZrC (typical)

HfN

The initial work utilized the MRC 902M$_2$ magnetron sputtering system to deposit HfN[3] onto M2 tool steel (Rc62), in order to determine the best range of deposition parameters. The first step in this evaluation procedure was to run

hysteresis curves. These curves were run at three different power levels, and the $N_2$ flow rate was measured at increasing (and then decreasing) values of $N_2$ partial pressure. The data is presented in Figure 14 for 3, 5, and 7 kW. Experience shows that the best operating conditions are near the knee (where the flow is a maximum and partial pressure increases dramatically) of the hysteresis curve.

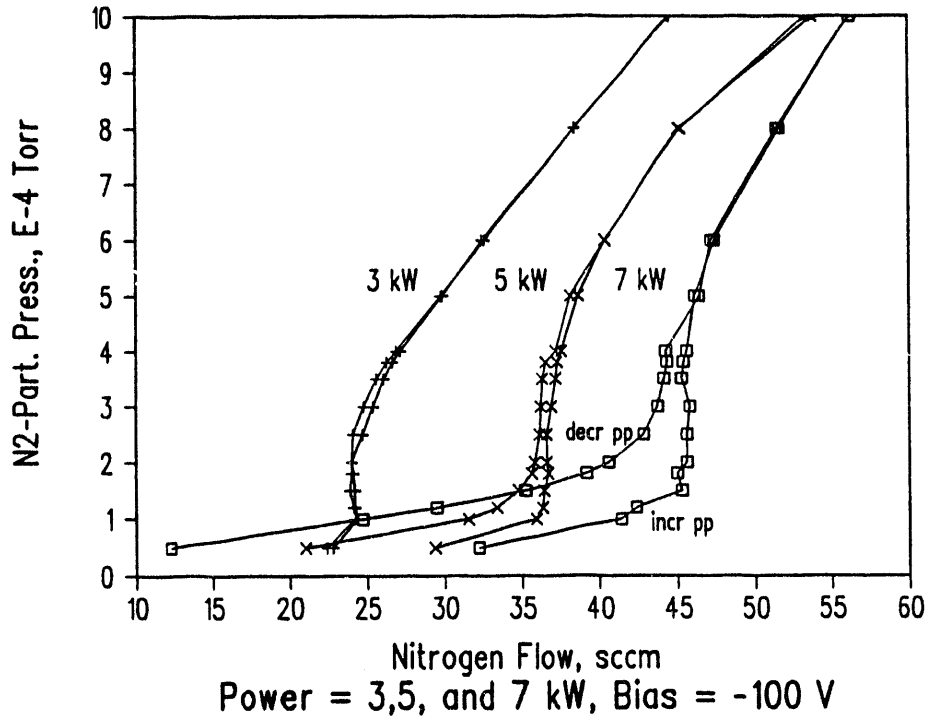


**Figure 14. HfN Hysteresis Curves - Partial Pressure Control**

Having determined the approximate operating conditions in terms of power and partial pressure, we set up a statistically designed experiment to determine the best operating conditions (evaluated in terms of hardness and adhesion). The response surface methodology was used with three independent parameters: power, nitrogen partial pressure, and substrate bias voltage. In the Box-Behnken design, three values were taken for each parameter and fifteen runs were made at thirteen different combinations of parameters (plus two duplicates). The parameter values selected for this experiment were: power =

3, 5, and 7 kW; partial pressure = 1, 1.5, and 2.0 x $10^{-4}$ Torr; bias voltage = -50, -75, and -100 V; and thickness = 5 $\mu$m.

The Vickers microhardness did not change very much with the deposition conditions and ranged from about 2900 - 3300 kg/mm$^2$ (on M2); whereas, the adhesion critical load (Lc) was quite sensitive and ranged from about 3 - 7 kgf. In the analysis of variance for the quadratic fit of the model curves to the data, the correlation of the hardness was very poor because of the small variations observed in hardness compared to the normal error in this measurement (approx. ± 10%). The correlation for the adhesion tests was fairly good (adj. R-squared = 0.73) because of the strong dependencies observed, but Lc is typically measured to only ± 0.5 kgf, making it difficult to get a model fit much better than we found here. The results of the statistical experiment for adhesion are shown in Figures 15-17.

Figure 15 is a perturbation plot that shows the general dependence of the adhesion-critical-load on each parameter. The factor (parameter) range is

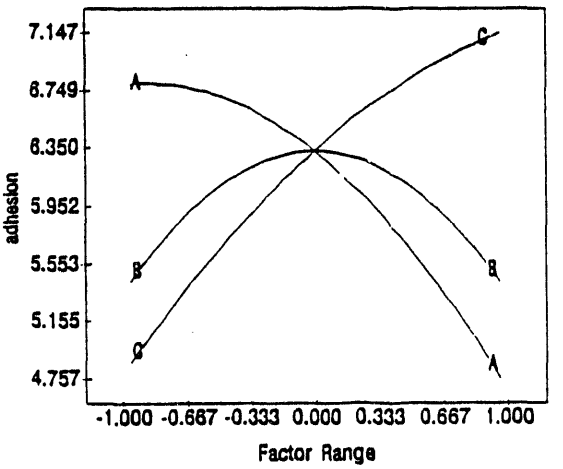


**Figure 15. Coded Perturbation Plot - Effect of Power (A), Bias Voltage (B), and $N_2$ Partial Pressure (C) on Adhesion Critical Load, Lc (kgf)**

coded so that the minimum and maximum of each parameter can be represented on the same plot. In this plot, the response for each parameter is tracked over the full range with the other parameters held at the centers of their respective ranges. The results are striking, showing the strong dependencies of adhesion on target power and partial pressure for the selected factor

values. The response to substrate bias voltage exhibits a maximum in the range we investigated.

The effect of the maximum is seen clearly in the three-dimensional plot in Figure 16. Here we have plotted the response (adhesion) on the vertical axis and power and bias on the other two axes. Partial pressure ($N_2$) is held constant at the highest value investigated (0.2 mTorr). The adhesion appears to be a maximum (Lc = 7 kgf) at a power of about 5 kW and a bias voltage of about -75 V.

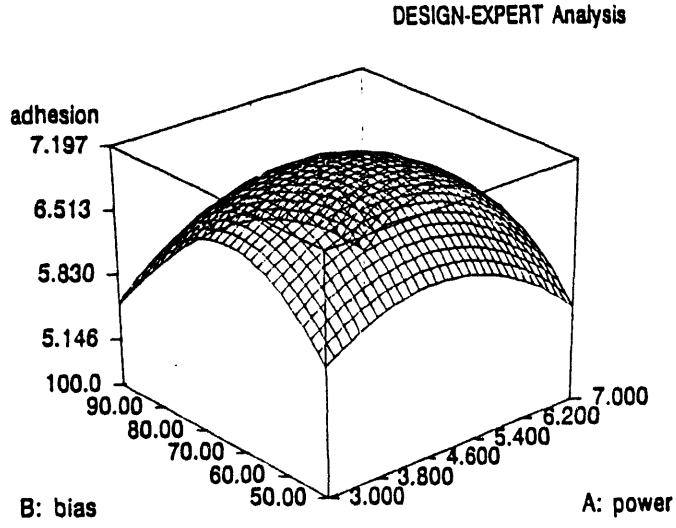


**Figure 16. Response Surface Plot - Adhesion Lc (kgf) of HfN vs. Substrate Bias Voltage (-V) and Power (kW)**

From Figure 15, we see that the adhesion has not yet reached a maximum in terms of the power and partial pressure values used here. The practical limit for the power, however, is 7 kW. The partial pressure can be further increased, and the response surface plot in Figure 17 indicates that we should be able to increase the adhesion by increasing the partial pressure of nitrogen while holding the bias at -75 V and the power at about 5 kW. In order to confirm this prediction, two more depositions were made: one at 0.25 mTorr and one at 0.30 mTorr, while holding the power and bias at the values indicated. The adhesion critical loads obtained were 8.0 and 7.0 kgf, respectively, indicating a relative maximum in adhesion at partial pressure of 0.25 mTorr of nitrogen. The hardness values were 3065 and 3180 $kg/mm^2$, respectively.

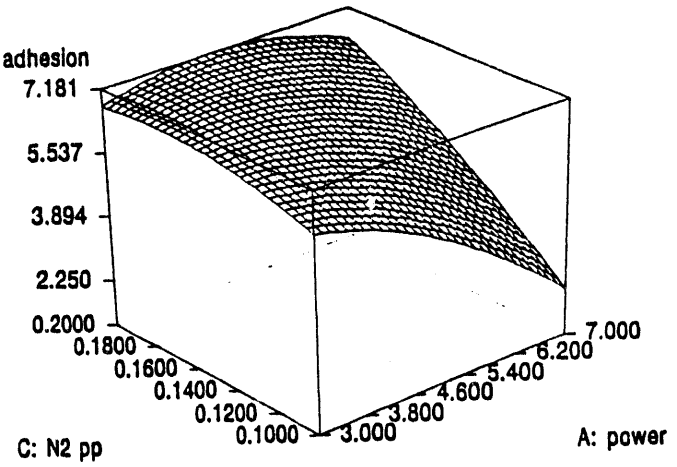


Figure 17. Response Surface Plot - Adhesion Lc (kgf) of HfN vs. Partial Pressure (mTorr) and Power (kW)

The deposition rate for HfN in this sputtering system was found to depend primarily on the target power. The nitrogen partial pressure also has an important effect, but the substrate bias voltage has a minimal effect on rate. This dependency on the two main parameters is shown in Figure 18. The use of partial-pressure control during the process enables us to maintain the maximum possible deposition rate at any power level. The highest rate of deposition

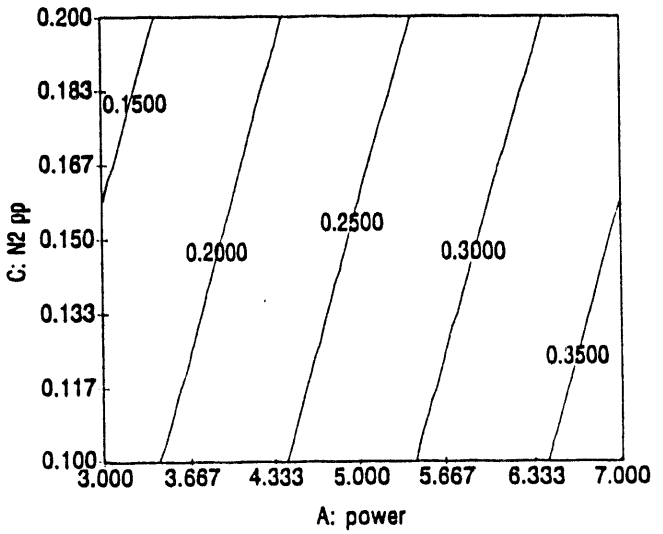


Figure 18. Response Surface Plot - Deposition Rate ($\mu$m/min) of HfN vs. Partial Pressure (mTorr) and Power (kW)

observed was about 0.37 μm/min at 7 kW and 0.1 mTorr $N_2$. At the highest explored partial pressure (0.2 mTorr), the rate dropped to about 0.32 μ/min. for the same power. The substrate bias was held at -75V for this plot.

The X-ray diffraction results confirmed that the films were HfN (cubic), although the texture and lattice parameter varied with the different operating conditions. The ratio of the (200) peak-intensity to the (111) peak-intensity ranged from 60% to 160%. The value of the (200) d-spacing also changed quite a lot over the different conditions, ranging from 2.23 to 2.95 Å. The value on the JCPDS card # 33-592 is 2.62 Å. Analysis of the lattice parameter data showed a systematic decrease in d-spacing with increasing nitrogen partial pressure, the same trend reported by Toth[4] for bulk $HfN_x$. The target power and substrate bias had secondary, but not insignificant, effects on the d-spacing of the coatings, as shown in the perturbation plot in Figure 19.

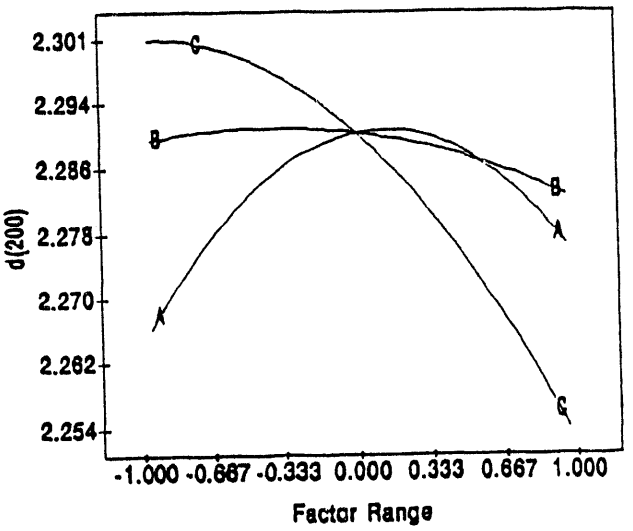


**Figure 19. Perturbation Plot - (200) d-Spacing of HfN vs. Power (A), Substrate Bias (B), and Partial Pressure of $N_2$ (C)**

A typical XRD curve is shown in Figure 20. This curve was recorded from a sample made at the conditions producing the best adhesion (8 kgf @ 5 kW power, -75 volts bias, and 0.25 mTorr $N_2$).

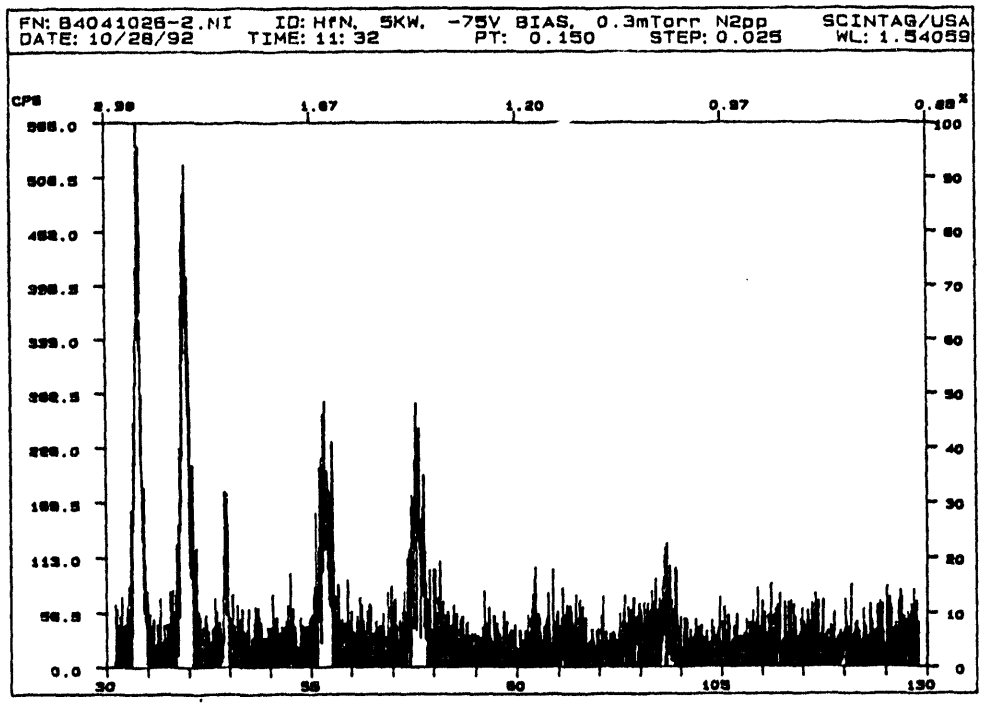


**Figure 20. X-ray Diffraction Pattern for HfN Deposited on M2 Steel. Power=5kW, Bias=-75V, and $N_2$-Partial Pressure=0.30 mTorr**

HfC

Hafnium carbide was deposited onto M2 steel in the same MRC 902-M system as the nitride. The reactive gas was changed from nitrogen to acetylene ($C_2H_2$). Based on previous experience with methane, it was noticed that the excess hydrogen build-up caused problems with the coatings and the process control. Acetylene improved this situation.

There was not sufficient time in the project to pursue the carbide deposition in the same depth that was used for the nitride. We did have prior experience, however, which we used as a guide. We could also use our work with ZrC as a guide since the two systems behave similarly. Consequently, we knew that it was not necessary to use partial pressure control, but the process could run with flow control. We also knew that the carbide would not adhere as readily to the steel substrate as the nitride does, therefore, we

put down an interlayer of HfN before depositing the HfC layer. This is the same procedure that was used for the ZrN/ZrC work.

Based on our prior work, we selected 6 kW power and 8 mTorr total pressure as the general operating conditions. The amount of acetylene and the substrate bias voltage were varied somewhat to determine the best operating conditions for making wear test samples. The total film thickness was about 4.5 $\mu$m, where the first 0.5 $\mu$m was HfN and the last 4.0 $\mu$m was HfC. The hardness generally ranged from 2500 to 2700 kg/mm$^2$, and the adhesion ranged from 1-3 kgf (Lc) on 52100 steel. These values changed with bias voltage (-50 to -100 V) and flow rate (26-30 sccm). The carbide was found to be more brittle than the nitride and, in general, gave lower adhesion critical loads. A few wear tests were run under the same test conditions as the HfN, but the starting friction was about 0.5 and the failure of the films began almost at the start of the test.

There was also some anomalous behavior noted for the HfC coatings in terms of measured adhesion and hardness. There seemed to be an aging effect (which was also reported in earlier work by Sproul[2]. That is, the hardness and adhesion values changed with time. For example, the adhesion for a particular sample was very low (Lc = 1.5 kgf) immediately after coating, but several days later the value of Lc increased to 3.0 kgf. Similarly, the hardness changed from about 1100 to about 3300 Vickers, as measured by the UMIS 2000 ultra-microindentation system. These numbers were measured using a 10-mN maximum force and may not be comparable to the usual microhardness values, but the relative values and changes in values are meaningful. After three months had passed, the same sample yielded adhesion and hardness values of 2.0 kgf and 2600 kgf/mm$^2$, respectively.

The UMIS load-unload vs. penetration curves (Figure 21) demonstrate more graphically the changes in properties for the three time periods. The aging process is not explained in this work, but it is evident that the properties of the carbide films are not stable for some time after deposition. These effects should be further explored.

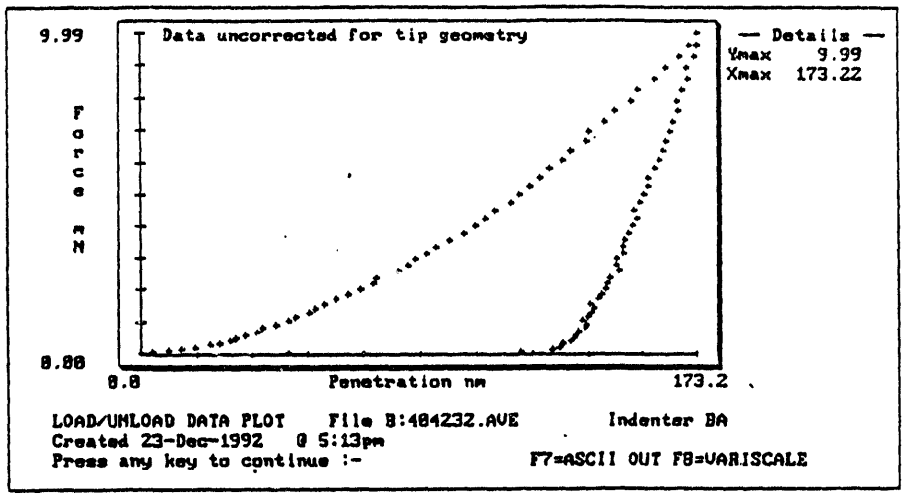


(a)

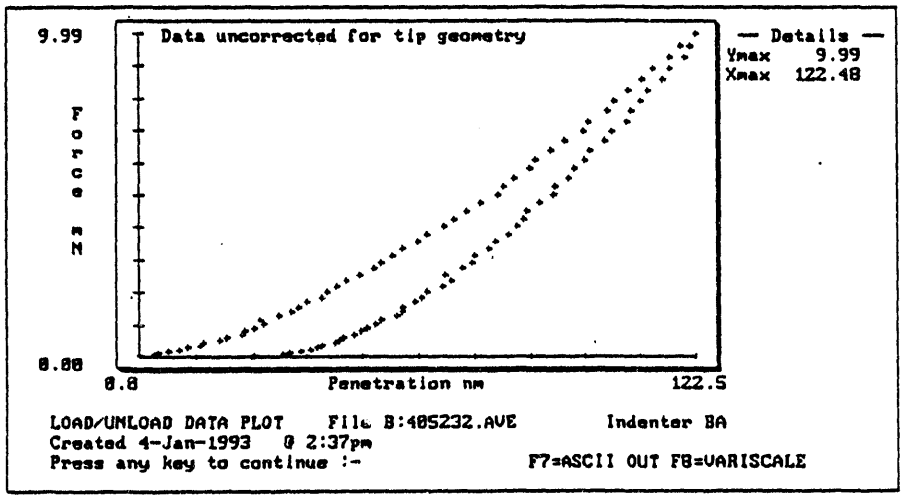


(b)

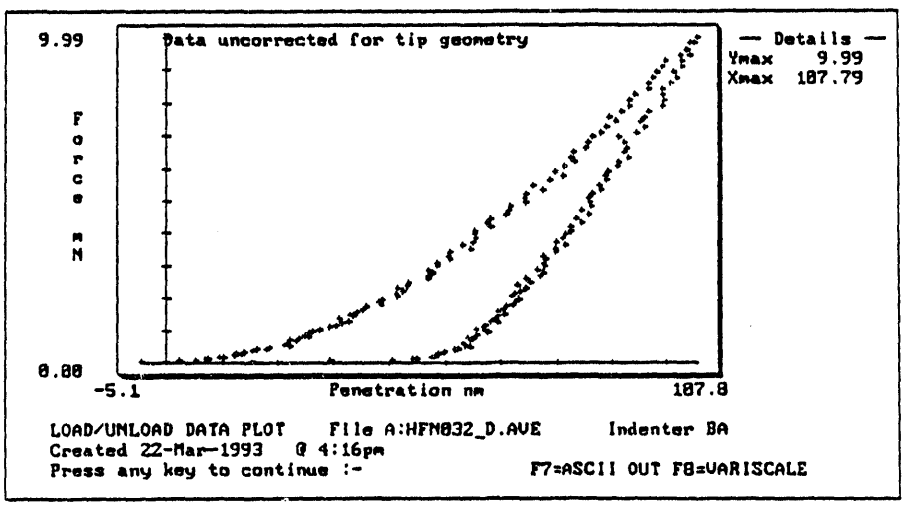


(c)

Figure 21. Ultra-microindentation Load-Unload, Force-Penetration Curves for HfC, (a) within one hour of coating, (b) after 12 days,and (c) after three months

## WEAR RESULTS

The wear testing of samples coated with TiN and TiC was undertaken by Peter Chang while he was still working on his Ph.D. degree under the guidance of Professor Herbert Cheng at Northwestern University. Later testing with ZrN, ZrC, HfN, and HfC was done at BIRL after Dr. Chang had joined our staff. The initial work focused on the effect of coatings on the contact fatigue failure of rolling and sliding surfaces. This work was very time-consuming but generated very valuable performance data for coated contacts (with TiN coatings). Later work was largely roller-on-roller scuffing and pin-on-disk wear testing. This change from rolling-contact-fatigue (RCF) testing was partly mandated by difficulties in scheduling the tester for such lengthy experiments. Broadening the scope of the investigation to include the effects of coating parameters and substrate characteristics provided other valuable information regarding the practical use of these hard coatings for wear resistance. Finally, as it became apparent that there would be no money available for the final year of the project because of a DOE cutback in funding, it was felt that it was necessary to use the most expedient means of testing in order to generate as much information as possible with the time and money remaining.

Most of the early work was done in Professor Cheng's laboratory using roller-on-roller type testing where the ratio of sliding and rolling could be controlled. The loading of the drive roller and the driven roller was controlled to obtain failures in the materials during a reasonable test time in the selected environment. The rollers were generally run with mineral oil lubrication maintained at a constant temperature (e.g., 80-100 °C), using a recirculating system. This test set up was used extensively to gain information on scuffing resistance and friction coefficients. Roller-on-roller testing was also used in the pure rolling mode to get rolling-contact-fatigue (RCF) data on the TiN films.

Among the parameters investigated for their effect on wear performance were deposition conditions such as reactive-gas partial pressure and substrate bias voltage. Since these parameters affect the chemical composition and the microstructure of the coatings, it was felt that they should be explored.

Other factors such as coating thickness, substrate hardness, and surface roughness would also have important effects on the wear performance, depending on the test environment. Correlations between these operating parameters or other easily measured properties such as hardness and adhesion and the wear resistance of the coatings was the goal for understanding the behavior of hard coatings and for being able to design coatings for specific applications. The results of these wear tests have all been reported in the Quarterly Progress Report, DOE-OTM Tribology Program publications through Argonne National Laboratory. As with the deposition data, the results will be summarized in this final report, but the Quarterly Reports should be consulted for further detail.

The following table summarizes the factors that were investigated, the test environment, and the coatings tested.

**Table 1. Coatings and Wear Testing**

| Factor Test | Composition (Partial Pressure) | Process Parameters (Bias,Power) | Thickness | Substrate Hardness | Substrate Roughness |
|---|---|---|---|---|---|
| Scuffing | TiN, TiC | TiN, ZrN | ZrN | TiN, TiC | TiN |
| Pin-on-Disk | TiN, HfN, HfC | TiN, HfN | HfN | | |
| RCF & Roll-Slide Fatigue | | | TiN | | |

## Rolling Contact Fatigue

An area of primary interest in this study was the effect of hard coatings on fatigue induced failure in wear environments. This includes rolling contact fatigue and scuffing in rolling/sliding applications. A thorough study of the effect of TiN coating thickness on fatigue life was undertaken. The test

samples were coated rollers run under lubricated contact conditions in the two-disk machine. TiN films of various thicknesses (0.25, 0.5, 0.75, 1.0, 2.5, and 5.0 $\mu$m) were deposited onto AISI 4118 steel rollers, by HRRS.

The degree of spalling on the coated surfaces was progressively monitored as the wear tests were run, providing information on the expected fatigue lives relative to coating thickness. The ratio of spalled area ($A_{sp}$) to the observed area ($A_{ob}$) was used as the fatigue damage index for different coating thicknesses at selected cycles. The experimental results revealed that a coating thickness of 0.25 $\mu$m gave the best fatigue resistance[5]. Both 0.25 and 0.5-$\mu$m thick films showed no measurable spalling after 60 million cycles, while the amount of spalling observed in thicker coatings increased with coating thickness (and number of cycles) as shown in Figure 22. The 2.5 and 5.0-$\mu$m films spalled severely and did not perform as well as the uncoated samples.

When the number of fatigue cycles to achieve a specific percentage of failure (eg., 5% or 10%) are plotted against the coating thickness, as in Figure 23,

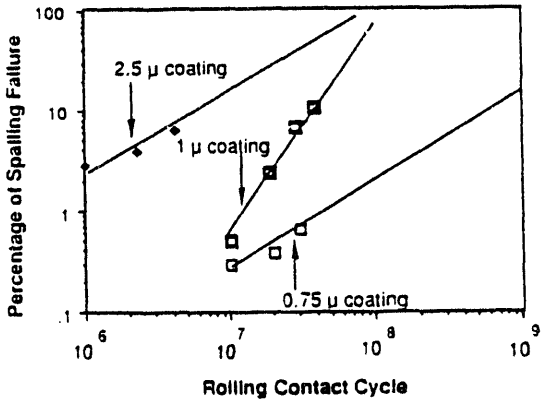


**Figure 22. Percentage of Spalling Failure vs. Rolling Cycles for Three Coating Thicknesses**

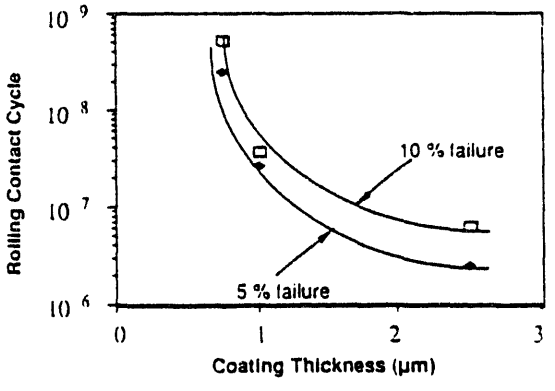


**Figure 23. Rolling Cycles vs. Coating Thickness for 5 and 10% Spalling Failure**

useful design information is generated for the engineer. The accumulated data on percent spalling was also used to show that the initial phase of spalling development was a relatively slow process, while the final growth of spalls lead to rapid failure of the contact surfaces.

Other studies[6] aimed at illuminating the nature of fatigue failures in rolling and sliding contacts were conducted on the two-disk machine using a roll:slide ratio of 4:1. Microstructural characterization of the worn surfaces and wear-track cross-sections revealed that the coated surface (1 $\mu$m TiN) deformed mainly elastically after 33 million cycles, whereas the uncoated surface showed significant development of subsurface cracking and surface spalling after only 10 million cycles. These results and the thickness effects previously described agree with the predictions of an analytical model by Kim, et. al.[7] Their theory calculated interfacial shear stresses and stress intensity factors for coated surfaces and predicted that the stresses would increase with coating thickness in much the same way that we observed in these experiments.

## Substrate Effects

While the main emphasis has been the study of the various coatings and their performance in different wear situations, it was also necessary to understand the effect of the substrate properties on the coating performance. In particular, it became evident that the hardness of the substrate (relative to the hardness of the coating) and the surface finish of the substrate would both play important parts in determining the successful application of a coating to a selected wear environment.

As noted in the TiC data, which will be reviewed in more detail later, the harder substrates performed better with the hardest coatings. The hard TiC material was able to realize its potential for low wear only when supported by material of sufficient strength. Work with the TiN coatings on various substrate hardnesses further revealed that, in fact, matching the coating and substrate hardness was important, since softer films could out-perform harder coatings if the substrates were relatively softer (than Rc 62).

For the TiN case, the coated and uncoated driven-rollers in contact with uncoated drive-rollers were tested in lubricated, rolling and sliding tests. One series of tests was run at a sliding and rolling speed combination of 121.48 and 97.42 m/sec, respectively. Another series of tests was run at a sliding and rolling speed combination of 151.81 m/sec. and 121.74 m/sec.,

respectively. All tests had a fixed slide-to-roll ratio of 1.247. The test lubricant was a mineral oil (no additives, with a viscosity of about 4.0 cst at 100°C) applied at a temperature of 100°C. The load was applied incrementally for each loading step until either scuffing failure occurred or the load limit on the scuffing tester was reached.

Three different hardnesses of the driven rollers (Rc 62, Rc 54, and Rc 45) were employed with a fixed Rc 62-hardness drive roller. The coating thickness was 1 $\mu$m. While the hardness could not be measured accurately on such thin films when this work was done, a relative measure of hardness was obtained from measurements on coatings deposited under the same conditions, although onto tungsten carbide substrates. The deposition conditions produced coatings with Vickers microhardnesses of about 3000 kg/mm$^2$ and 2200 kg/mm$^2$. The substrate hardnesses were not changed during the deposition of the coatings.

Figure 24 summarizes the data and dramatically shows the increase in scuffing load that is possible when the correct combination of coating and substrate hardness is achieved. From this figure, one can see the advantage of using a relatively hard TiN film (coating A) for a relatively hard substrate (Rc 62).

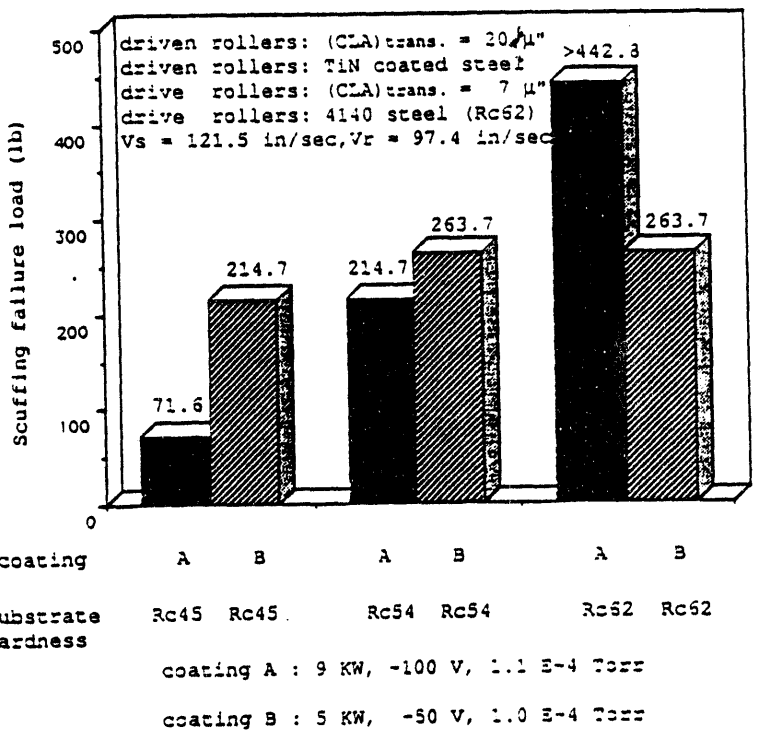


**Figure 24. Scuffing Failure Loads vs. Substrate Hardness for Two Different Hardnesses of TiN Coatings**

In this case, the scuffing failure load has been increased at least ten times with the use of coating A. For the relatively soft substrate (Rc 45), it is better to apply the softer TiN film (coating B) in order to obtain the protection of titanium nitride from early scuffing failure. The coating parameters, target power, substrate bias voltage, and nitrogen partial pressure are given in the figure for each coating.

The post-test examinations showed that coating-B, on substrates with hardnesses of Rc 54 and Rc 62, was still intact prior to scuffing failure. For coating-B on the substrate with a hardness of Rc 45, the coating delaminated before scuffing, as it did for the harder coating on both the Rc 45 and Rc 54 substrates. From these experimental results, one can conclude that hard coatings can be beneficial when deposited onto steel substrates, but the match of mechanical properties of the materials involved is crucial for optimum results.

The surface finish of the wear sample also affects the performance of the coating. The influence of surface roughness on the tribological behavior of TiN-coated steel rollers has been investigated with a roller-on-cylinder tribo-tester. Driven rollers of various surface roughnesses were coated with 1-$\mu$m TiN coatings by HRRS. In the case of the rougher surfaces, 2 and 3-$\mu$m coatings were also applied to see if the effect of roughness could be mitigated by the use of thicker coatings.

Figure 25 shows the scuffing failure load of coated and uncoated driven rollers with various surface roughnesses. For relatively smooth surfaces (Ra=0.25 and 0.50 $\mu$m) the scuffing lives of steel substrates were significantly increased with the TiN coatings. For these cases, failure did not occur within the load limit of the test machine. For relatively rough surface conditions (Ra=0.88 and 1.5 $\mu$m), the scuffing failure loads for coated driven rollers were only slightly higher than for uncoated rollers. Progressive examinations during the rolling/sliding tests showed that the TiN coatings on the rougher surfaces had delaminated prior to the occurrence of scuffing failure. The use of thicker (2 and 3 $\mu$m) coatings did not improve the performance on these rougher surfaces, which suggests that the surface roughness dominates the scuffing behavior above certain roughness levels.

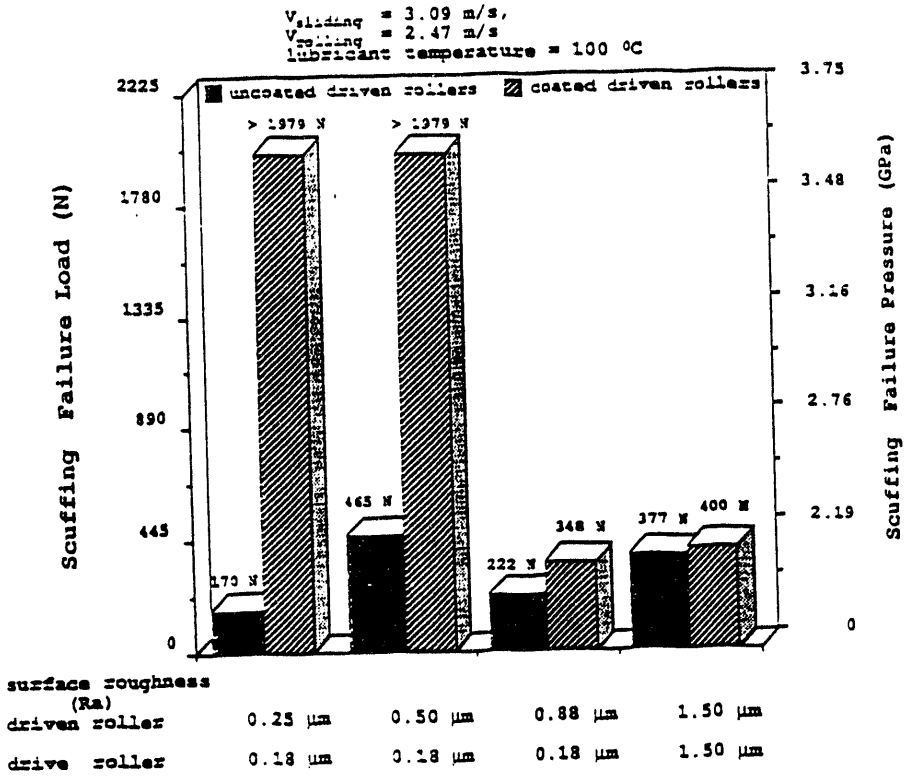


**Figure 25. Scuffing Failure Load of TiN-Coated and Uncoated Rollers vs. Surface Roughness**

Another fact that emerged in this and other studies was that the wear performance (especially scuffing tests where load is increased to achieve failure) may depend on the products of the wear process. Often it was found that the wear life was extended and the friction was reduced by the generation of an oxide-debris layer on the surfaces of the wear couple. The presence of the nitride coating often enabled the surfaces to resist scuffing long enough to experience the higher loads and temperatures necessary to form the oxide layer. This oxide layer would then act like a solid lubricant for the system.

## Processing Effects

Coating composition is altered primarily by changing the partial pressure of the reactive gas in the sputtering system. Compositional variations also affect the hardness and adhesion of the coatings so that there is no simple correlation with the wear-test results (for this or any other parameter effects).

Recognizing the importance of stoichiometry in producing good quality coatings, research was conducted on the tribological properties of different TiN films by means of scuffing tests. The influence of target power, $N_2$-partial-pressure and substrate bias-voltage on scuffing and related behavior was experimentally investigated using a roller-on-cylinder scuffing tester. A drive roller (3.84 cm diameter with a 1.78 cm crown-radius) was made from 4140 steel. The rollers were case-hardened to a thickness of 1.0 mm, with a case hardness of Rc 60-62, and a core hardness of Rc 38-40. The driven roller (1.91 cm diameter with no crown radius) was made of 52100, through-hardened steel, with a hardness of Rc 60-62.

As shown in Figure 26, one of the TiN films (Case A) exhibited good scuffing resistance. Scuffing occurred at a load of 263 N, which was more than twice

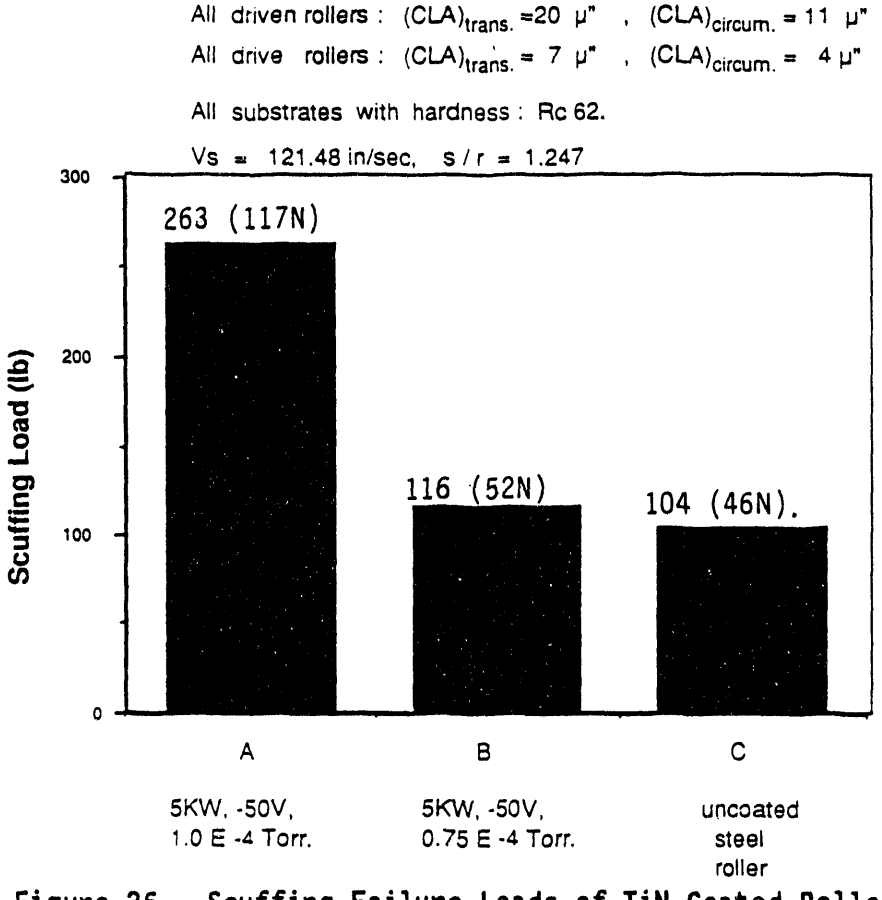


**Figure 26. Scuffing Failure Loads of TiN-Coated Rollers vs. Nitrogen Partial Pressure (Composition of the TiN)**

that of the uncoated roller. A films made at a lower partial pressure of nitrogen (Case B) scuffed at lower loads, nearer to the failure load of uncoated steel (Case C). The differences in response are attributed to differences in the nitrogen partial pressure since the other deposition conditions were constant. The use of higher substrate bias (-100 V) improved the performance such that the 1.0 E-4 Torr-$N_2$ coating did not fail within the limits of the machine (198 N). The higher substrate biases also contribute to the superior performance by creating denser, harder microstructures.

It has also been suggested that non-stoichiometry can affect the density. In fact, Sundgren[8] has reported that in a stoichiometric TiN film, no voids can be observed, whereas the non-stoichiometric films possess voids located in the grain boundaries and produce a lower-than-optimum density. For both under-stoichiometric and over-stoichiometric films, a lower density can be found. Voids are weak points where crack propagation and fracture are initiated as external forces are applied. Non-stoichiometric TiN films, possessing voids located in grain boundaries, have lower strength and hardness and will promote cohesive failure under an applied, concentrated contact.

We also investigated the effect of composition on the wear resistance of titanium carbide coatings[9]. TiC coatings were deposited on test rollers by the high-rate-reactive magnetron sputtering technique. Three different reactive-gas ($CH_4$) flow rates (20, 30 and 50 sccm) were used for 1-$\mu$m thick TiC coatings, with the power (9 kW), total pressure (8 mTorr), and the substrate bias (-100 V) held constant. The deposition temperature was lower than 200°C, and there was no significant change of substrate hardness after deposition. Driven rollers (52100 steel) with three different hardnesses (Rc62, Rc54, and Rc45) were coated and tested against a drive roller (4140 steel) of hardness Rc62. While the coating properties were not measured directly on these test rollers (the coatings were too thin for reliable hardness measurements), other work, on thicker coatings, indicated that the hardness ranged from 720-1100-3000 VHN for coatings made under similar conditions and flow rates as used here (20, 30, and 50 sccm, respectively). The lowest hardness was about equivalent to the substrate hardness of the drive roller (Rc62).

The reactive-gas flow rate, the driven-roller substrate hardness for each contact pair, and related test result are summarized in Table 2. As shown in the table, contact-pairs A,B,C and D did not scuff within the load limit of the test machine. Wear track profiles were measured with a profilometer, perpendicular to the sliding direction, to obtain the wear scar area. Such profiles showed that even though scuffing failure was not triggered for pairs A,B,C and D, their wear characteristics varied greatly, depending on the coating

**Table 2. TiC-Coating Test Conditions and Results**

| Contact Pair | Reactive-Gas Flow Rate (sccm) | Driven-Roller Substrate Hardness (Rc) | Scuffing-Failure-Load (N) | Wear Scar Area of the Driven Roller ($\mu m^2$) |
|---|---|---|---|---|
| A | 50 | Rc45 | >1979 | 9876 |
| B | 50 | Rc62 | >1979 | 770 |
| C | 20 | Rc62 | >1979 | 2426 |
| D | 30 | Rc54 | >1979 | 4071 |
| E | 20 | Rc54 | 1450 | Severe damage |
| U54 | Uncoated | Rc54 | 530 | Severe damage |
| U62 | Uncoated | Rc62 | 131 | Severe damage |

conditions and the relative properties of the coatings and their substrates. For contact-pair E, with the same substrate hardness as that of pair D, but different coating conditions, scuffing failure occurred at 1450 N.

In general, among the tested samples, it appears that the harder substrates perform better and that the coatings with higher carbon levels (higher flow rates of reactive gas) perform better. However, as the results also show, the interactions of the coating, the substrate, and the wear environment produce a complicated response. There is no doubt that good TiC coatings can perform well and can provide superior tribological properties compared to those of uncoated steel substrates.

Profilometer traces were made on both the coated and uncoated rollers after testing. The results of the wear on the uncoated drive rollers are not shown in the table since they were not quantitative, but the degree of wear followed the expected pattern. That is, the hardest coatings on the hardest substrates produced the most wear on the uncoated drive roller, while showing the least wear themselves. The softer coatings on softer substrates caused less wear on the uncoated drive rollers. The uncoated rollers were machined with a crowned contact surface so that, to the degree that this crown was worn by the hard counterface, the contact area and the contact stress was reduced, producing less wear in the coated surface. The softer coatings and substrates had less effect on the shape of the crown and were themselves worn substantially more.

In all cases, some of the coating was worn through but some remained in the wear track at the end of the test. To the extent that the coating was left intact it could not only resist scuffing but could support the formation of lubricous oxide films (due to high temperatures during the wear process) that lowered the overall coefficient of friction during the course of the test. In contrast, the uncoated samples would scuff before the conditions for generating the oxide films could be achieved.

The curves in Figure 27 show the friction behavior of the coated substrates during the tests as a function of the applied load. In addition to the

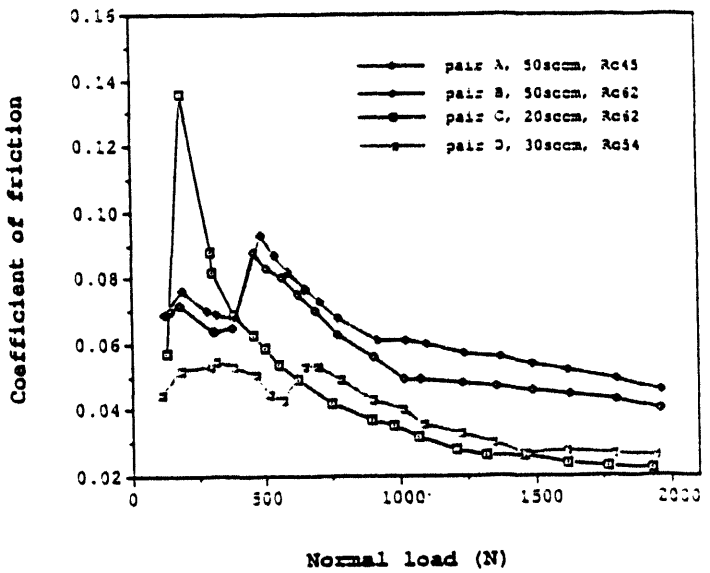


Figure 27. Friction Behavior During Scuffing Tests of TiC-Coated Rollers

general decrease in the friction coefficient, there is an initial sharp increase that appears to correlate with the loss of coating. The long term friction values appear to decrease the most for samples where more of the coating is worn away. This may be the effect of exposing more steel, or earlier formation of oxides because of more severe wear. The better wearing coatings exhibited somewhat higher friction at the end of the test, but it was still quite low. In general, it was observed that these hard coatings performed very well in lubricated wear conditions, showing much lower wear and much lower friction than the uncoated case.

Similar results have also been reported for our coatings by the tribology group at Argonne National Laboratory. Some of this work has been reported in the literature[1] , but not all the samples provided to Argonne under this contract have been tested yet.

Zirconium nitride (ZrN) coatings have been deposited on wear-test rollers by the high-rate-reactive magnetron sputtering technique.[10] Three different coating thicknesses of ZrN (0.25, 0.63 and 1.0 $\mu$m) were applied to AISI 52100 steel substrates of hardness, Rc 62. The other deposition conditions were held constant for this series, using the MRC 902-M magnetron sputtering system. The conditions were as follows: target power = 8 kW; substrate bias voltage = -150 V; total pressure = 8 mTorr; partial pressure of $N_2$ = 0.4 mTorr. A 0.25-$\mu$m thick ZrN layer was also deposited using a substrate bias voltage of -50 V. The deposition temperature was lower than 200°C, and there was no significant change of substrate hardness after deposition.

It is noteworthy that the deposition conditions used for these wear-test samples are different from the best values found in a later statistically designed experiment (presented earlier in this report). Specifically, the nitrogen partial pressure of $0.4 \times 10^{-4}$ Torr is more than twice that found in the later study ($0.175 \times 10^{-4}$ Torr). The particular rotation device used to coat the wear samples limited the pump-down time, and forced us to operate the system while the base pressure was still an order of magnitude higher than that normally used (normal = $0.5\text{-}1.0 \times 10^{-6}$Torr). The operating conditions were picked based on the achievement of what we decided were acceptable properties; that is, color, hardness and adhesion on a polished M2 block. The measured

values of hardness and adhesion critical load were 2340 VHN and 5 kgf, respectively, for a 5-$\mu$m thick coating.

The scuffing resistance of the ZrN-coated driven rollers was tested in contact with uncoated drive rollers in lubricated, combined rolling and sliding conditions. The tests were run at sliding and rolling speeds of 3.86 m/s and 3.09 m/s, respectively. The circulating lubricant was a mineral oil supplied at a temperature of 80°C. The load was applied incrementally until either scuffing occurred or the load limit of the test machine was reached.

The scuffing test results are summarized in Table 3. All the contact pairs failed within the load limit of the test machine (1979 N). However, the ZrN

**Table 3. Scuffing Resistance of ZrN-Coated Rollers Run Against Uncoated Steel Rollers**

| Contact Pair | ZrN Coating Thickness ($\mu$m) | Substrate Bias (V) | Scuffing Failure Pressure: GPa; Load: (N) |
|---|---|---|---|
| A | 1.0 | -150 | 3.5 (1797) |
| B | 0.63 | -150 | 3.5 (1797) |
| C | 0.25 | -150 | 2.7 (825) |
| D | 0.25 | -50 | 3.0 (1132) |
| E | uncoated | | 1.5 (141) |

coated pairs significantly increased the scuffing failure load of the steel rollers. Pairs A and B with the ZrN thicknesses of 1.0 and 0.63 $\mu$m, respectively, scuffed at a load of 1797 N, which was more than 13 times that of the failure load of an uncoated contact pair. ZrN coated rollers, with a coating thickness of 0.25$\mu$m, did not perform tribologically as well as rollers with thicker coatings.

The steel substrates had a surface roughness of 0.25$\mu$m Ra, and it is believed that such roughness contributes to the earlier failure of very thin films since the underlying material cannot adequately support the film at the points of

contact. While the thicker films are stronger, even they would do better with a smoother substrate. The sputtered coatings do not level the surface, but generally replicate it. Thus, the scuffing test is sensitive to film thickness because it affects the strength or load-carrying capacity of the film. Previous studies have shown that for other wear mechanisms, such as rolling contact fatigue, the performance shows a different dependence on coating thickness, and the optimum coating thickness may be less than one micron.[11]

Test rollers with the same coating thickness (0.25$\mu$m), but different substrate bias voltages, scuffed at different failure loads. The roller with the higher bias (-150V), had the lower scuffing failure load. A plausible explanation for this behavior is that the higher bias voltage caused the coating to be more brittle and more highly stressed than did the lower bias condition. The film properties such as hardness and adhesion were not measured directly on these samples because of the surface roughness and the thinness of the coatings. Prior work shows that for near-stoiciometric films, both hardness and adhesion (Lc) at first increase with increasing bias, to maximum values, and then decrease. The deposition parameters for the observed maxima for hardness and adhesion do not necessarily coincide, and the optimal conditions may require a compromise for both properties. Adhesion (Lc) for 5-$\mu$m coatings (on a polished witness sample), made under the present conditions, was typi-cally in excess of 5 kgf, and the hardness was typically greater than 2000 HV.

Basically, during the sputtering process, an increase in applied substrate bias voltage increases the energy of the ion bombardment on the growing film. While the increase in energy acts to densify the microstructure and to produce harder films through microstructure refinement and production of internal stress, in the extreme case, the bombardment produces excessive stress that reduces the ductility of the films and adversely affects their adhesion to the substrate.

## Correlation of Wear with Hardness and Adhesion

Pin-on-disk wear tests were run on the HfN coated 52100, hardened-steel samples under dry sliding conditions.[3] We wanted to determine any correlation between the measured adhesion (scratch test) and hardness and the wear results. Dry sliding of coated pins against coated disks, under fairly severe conditions (50

rpm, 9.1 kgf) allowed us to differentiate the various coatings according to their wear performance. Table 4 summarizes the wear test results and includes the deposition conditions and measured hardness and adhesion (on polished witness samples of the same 52100 material).

**Table 4. Summary of HfN Pin-on-Disk Wear and Related Data**

| $N_2$-Partial Pressure $xE^{-4}$ Torr | Bias (-V) | Micro-Hardness (25g) ($kg/mm^2$) | Adhe-sion Lc (kgf) | Thickness ($\mu m$) | Friction coeff. @ start | Time @ f-increase (min) | Pin-wt. loss (mg) |
|---|---|---|---|---|---|---|---|
| 2.5 | 50 | 2400 | 5.5 | 3 | 0.15 | 18.9 | 0.12 |
| 2.5 | 75 | 2716 | 4.5 | 3 | 0.20 | 9.2 | 0.35 |
| 2.5 | 75 | 2970<br>2960 | 4.0<br>4.5 | 5<br>5 | 0.15<br>--- | 5.4<br>4.9 | 1.3<br>2.3 |
| 2.5 | 100 | 2800 | 4.5 | 3 | 0.20 | 4.4 | 1.1 |
| 3.0 | 75 | 2890 | 5.0 | 3 | 0.2 | >20 | 0.09 |
| 3.5 | 75 | 2890 | 4.0 | 3 | 0.22 | 5.6 | 0.49 |
| uncoated<br>52100 | ----<br>---- | ------<br>------ | --------<br>---- | -------- | 0.15<br>0.15 | 2.7*<br>2.4* | 0.-<br>32**<br>0.41 |

* - The uncoated samples exhibited an increase in coefficient of friction at this time during the test beyond the gradual increase that occurred with running time. For the last half of the 20-minute test period, the uncoated sample pairs showed a coefficient of friction of 1.0 - 1.2. The coated samples were allowed to run for twenty minutes, but the times recorded in this column are those times where there was a significant jump in f, indicating some failure of the coating.

** - Pin weight-loss is an end-point measurement and corresponds to the weight loss after 20 minutes time, regardless of the time to cause film failure, except for this sample, which was run for only 16.5 minutes.

The results appear sensible since the films with the best adhesion gave the best wear results. In the series of 3-$\mu$m coatings made at an $N_2$ partial pressure of $2.5 \times 10^{-4}$, the hardness increased with substrate bias voltage (-V), but the adhesion (Lc) was best at the lowest hardness, as was the wear resistance. Increasing the partial pressure of $N_2$ to $3 \times 10^{-4}$ Torr improved the hardness and the wear resistance, with only a slight loss in Lc. A further increase in the partial pressure of $N_2$ reduced the adhesion and the wear resistance.

A 5-$\mu$m coating measured harder (greater thickness means less substrate effect on the measured hardness, and also increased internal stress) than the 3-$\mu$m film but did not improve the wear performance. In fact, in two separate tests, the measured wear resistance was worse than that obtained for the 3-$\mu$m coating. The higher internal stresses may have promoted the early failure.

Finally, we note that when the film failed prematurely, the wear rate on the pin was greater than it was for an uncoated pin against an uncoated disk. In addition, a significant wear track was observed on the coated disk, indicating that the coating was also failing on this surface.

A few wear tests were run for HfC coatings under the same test conditions as the HfN. The starting friction was about 0.5 and the failure of the films began almost at the start of the test. There was insufficient time to explore the carbide coatings satisfactorily, and more work should be done to improve the processing conditions for sputtered carbide coatings. As noted in the discussion of the deposition of HfC, there are questions about the microstructural stability of the films.

## CONCLUSIONS

While the original aims of this study involved a general determination of the effect of nitride and carbide coatings on the wear behavior of hardened steel, the results of the work have shown more specifically that many aspects of the coating-substrate system are important in determining the success of failure of coated surfaces in tribological environments. In discovering how to make the best coatings of each composition for wear testing, it was necessary to

determine the optimal deposition parameters. It was also necessary, for any wear test, to determine the effect of coating thickness, surface roughness, and substrate hardness. Finally, as a practical matter it was desirable to determine the correlation, if any, between the wear behavior and the measured properties such as hardness and adhesion. This relationship was found to be dependant on system variables such as substrate hardnesses of the wear couples, but within a selected wear system, the relative importance of adhesion and hardness were demonstrated.

We have more experience with the processing of the nitride materials and were able to obtain better results with them in general. However, both the nitrides and carbides were found to improve the wear performance of the steel by significant (often order of magnitude) factors. Different compositions and different deposition conditions will be best suited to different applications, but in general, these coatings have proven to be beneficial for dry sliding, lubricated sliding, rolling, and mixed rolling/sliding wear environments.

Among the important findings are the results of the rolling contact fatigue studies that showed the remarkable improvements of lifetime that could be achieved with very thin coatings (less than one micron). Thicker coatings were not found to be useful. This is an area where more study and correlation of experimental and theoretical modeling would be valuable. With a proper understanding of the mechanism of this effect, we could better predict the effects of hard coatings for such applications.

The finding that the coating and substrate properties (hardness) should be matched for the best performance also opens new research possibilities. The protection of substrate materials that are softer than fully-hardened tool steel is a goal for many applications. While the results may not be spectacular yet for hard coatings on soft substrates, it appears that there is much we can do to improve the situation by applying coatings of "appropriate hardness" for a given substrate.

Finally, we have demonstrated that the properties and performance of the hard coatings are controlled by the process parameter settings and that these

parameters can be effectively controlled in magnetron sputtering to achieve excellent results. Friction and wear can be effectively controlled in many applications through the judicious use of thin, hard, sputtered coatings.

## References


1. O. O. Ajayi, et al., Surf. Coatings and Technology, **54/55** (1992), pp. 496-501.

2. W. D. Sproul, J. Vac. Sci. Technol., **A4 (6)**, Nov/Dec (1986) p. 2874.

3. M.E.Graham, W.D. Sproul, T.P. Chang, and H.S. Cheng, Semiannual Progress Rpt., DOE-OTM Tribology Program, Oct.1992-Mar.1993 (ANL/OTM - 93/1).

4. L. E. Toth, Transition Metal Carbides and Nitrides, Acad. Press, N.Y. (1971), p. 90.

5. W. D. Sproul, H. S. Cheng, and T. P. Chang, Quart. Progress Rpt., DOE-OTM Tribology Program, Jul.-Sept. 1990, p. 153 (ANL/OTM--90/1).

6. Ibid., 1, Apr.-Jun. 1990, p. 153 (TRIB/ECUT--90/3).

7. S.H. Kim, L.H. Keer, and H.S. Cheng, STLE Transactions, **33**, (1990), p. 53.

8. J. E. Sundgren, Thin Solid Films, **128** (1985), pp. 21-44.

9. W. D. Sproul, M. E. Graham, T. P. Chang, and H. S. Cheng, Semiannual Progress Rpt., DOE-OTM Tribology Program, Oct.-Mar. 1992, p. 105 (ANL/OTM--92/1).

10. T. P. Chang, W. D. Sproul and M. E. Graham, Semiannual Progress Rpt., DOE-OTM Tribology Program, Apr.-Sept. 1992, p. 120 (ANL/OTM--92/2).

11. T. P. Chang, H. S. Cheng, W. A. Chiou, and W. D. Sproul, Tribology Transactions, STLE, **34**, 3 (1991), pp. 408-416.

DATE
FILMED
8/3/94
END